Investigating the potential of *Plantago major* in the removal of PFAS from soils and surface waters

Aaron van Adrichem

Student number: 6464696

MSc Thesis

Department of Earth Sciences

Earth Surface and Water

Supervisors

Dr. Lubos Polerecky (Utrecht University)

Marc Verheul (Deltares)

May 2024

Summary

The occurrence of per- and polyfluoroalkyl substances (PFAS) in environmental media, such as soils and surface waters, has led to a worldwide concern. This is because most PFAS have a tendency to accumulate in organisms, potentially leading to toxicity. Currently, conventional remediation techniques, such as sorption and chemical treatments, are costly, have adverse environmental effects, and are not viable for large-scale projects. Phytoremediation, or the use of plants for environmental cleanup, is a potentially low-cost and environmentally friendly technique that is suitable for large-scale PFAS remediation from soils and surface waters. This study aimed to investigate whether perfluorooctanoic acid (PFOA) and perfluorooctanesulfonic acid (PFOS) can accumulate in plant tissues (leaves, stems, and roots) under UV light exposure, and whether subsequent degradation of these compounds occurs. Plants of the species *Plantago major* were grown for a maximum of 28 days in two separate fume hoods each with a different light regime. One fume hood was equipped with a UV-light (UV-A + UV-B) and a white growing light, while the other fume hood only contained a growing light. The plants were cultivated in nutrient solutions containing spiked ^{13}C labelled PFOA and PFOS, at two concentrations of 2.5 µg/L and 25 µg/L. The effect of UV light and PFAS exposure on the health of plants was assessed visually and by determining the net biomass gain, i.e., the difference between the initial and final wet mass as a proxy for plant growth. The $\delta^{13}C$ (‰) value of the plants was determined using EA-IRMS as an indicator for the bio-accumulation of PFOA and PFOS in the tissues of *Plantago major*. NanoSIMS was used to determine the spatial distribution of accumulated PFAS in the plant tissues and to investigate whether PFAS degradation occurred in the plants. The majority of plants remained healthy throughout the study period. Visually, no significant difference was visible in color, morphology, and growth between exposed (UV and/or PFAS) and non-exposed plants. The net biomass gain did not significantly differ between UV treated and non UV treated plants. Additionally, no significant correlation was observed between the net biomass gain and the PFAS treatment the plants received. This indicates that the plant growth and health is not significantly affected by UV-light and the presence of PFOA and PFOS in the nutrient solution. Also no significant correlation between the $\delta^{13}C$ value and the treatment was found. The biological variability of this values

exceeded the potential increase in $\delta^{13}C$ due to PFAS, which made it impossible to differentiate between PFAS incorporation into the tissues and natural biological variability. Analysis of both $^{13}C/^{12}C$ ratios and $^{19}F/(^{12}C+^{13}C)$ ratios in plant tissues, obtained via NanoSIMS analysis, revealed possible accumulation of both PFOA and PFOS in the leaves of several plants. Interestingly, elevated ratios were also detected in a leaf of a plant that did not receive UV or PFAS treatments. However, most samples did not exhibit enhanced $^{13}C/^{12}C$ ratios and/or $^{19}F/(^{12}C+^{13}C)$. Therefore, the elevated ratios in some of the samples cannot solely be attributed to PFAS accumulation in plant tissues. Given the uncertainty surrounding the accumulation of PFAS in the plants, further interpretations concerning the potential degradation of PFAS within the plant tissues (leaves) were abstained from.

Contents

Introduction **4**

Literature review **7**

1. PFAS 7
2. PFAS contamination 11
3. Phytoremediation 27

Methods **32**

1. Chemicals 32
2. Plant collection and preparation treatment 32
3. Experimental design 33
4. Growth of *Plantago major* 35
5. Bulk analysis 35
6. NanoSIMS analysis 39
7. Data visualization and statistical analysis 41

Results **42**

1. Growth of *Plantago major* 42
2. Bulk analysis 45
3. NanoSIMS analysis 48

Discussion **54**

1. Interpretation of the results 54
2. Limitations of the study and future directions 63

Conclusions **66**

References **67**

Appendix **76**

Introduction

Following the completion of his doctorate at Ohio State University, Roy. J. Plunkett began investigation on new chlorofluorocarbon refrigerants at the chemical company DuPont. In 1938, he and his associates produced hundred pounds of tetrafluoroethylene gas (TFE), which they then stored in small cylinders at temperatures of around -100° C. When Plunkett opened the cylinders for further use, he discovered that the gas had polymerized into a white waxy powder to form polytetrafluoroethylene (PTFE). Plunkett found the solid to be heat resistant, very durable and inert to virtually all chemicals. Furthermore, the substance was extremely slippery and was considered the most slippery substance known to man (Roy J. Plunkett | Science History Institute, n.d.); (The History of TeflonTM Fluoropolymers, n.d.). Today, PTFE, commonly known by its trademark Teflon, has nearly 40 applications in various industries (Glüge et al., 2020).

The chemical Teflon is part of a broad group of synthetic substances called PFAS or poly- and perfluoroalkyl substances. Although there is no universally accepted definition for PFAS, the Organisation for Economic Co-operation and Development (OECD) defines PFAS as "fluorinated substances that contain at least one fully fluorinated methyl or methylene carbon atom (without any H/Cl/Br/I atom attached to it), i.e., with a few noted exceptions, any chemical with at least a perfluorinated methyl group (–CF3) or a perfluorinated methylene group (–CF2–) is a PFAS". The presence of extremely polar C-F bonds makes most PFAS exhibit (1) high chemical stability, (2) high thermal resistance, and (3) resistance to biotic degradation (Shahsavari et al., 2021). Besides these properties, PFAS typically possess a hydrophobic fluorinated "backbone" and a hydrophilic functional group. This combination of hydrophobic and hydrophilic components make most PFAS surface-active, or surfactants (Banayan Esfahani et al., 2022). Due to their unique physico-chemical properties, PFAS are commonly used in a variety of industrial, commercial and consumer applications, dating back to at least the 1950s. Common applications in which PFAS are processed include fire-fighting foams, cosmetics, adhesives, non-stick cookware, water- and oil-repellent coatings and (food) packaging (Gaines et al., 2023).

Because of its extensive use in many applications, PFAS are being released and detected nearly everywhere in the natural environment. PFAS are detected in varying concentrations in air samples, aqueous matrices, abiotic solid matrices, wildlife and humans (Nakayama et al., 2019). PFAS concentrations in aqueous environments typically range from pg/L to ng/L. However, high PFAS concentrations (µg/L to mg/L) have been detected in surface waters and groundwaters, due to firefighting activities, explosions or chemical disposal of fluorochemical manufacturing industries (Banayan Esfahani et al., 2022).

The release of PFAS to the environment has led to significant global concern, since many PFAS tend to accumulate in biota, potentially leading to toxicity (Lewis et al., 2022). Although the toxicological effects of PFAS in humans are complex, PFAS have been associated with the formation of cancer, immunotoxicity, impacts on metabolic processes, and neurodevelopmental effects (Sunderland et al., 2018).

Due to these potential health risks posed to humans, coupled with their environmental persistence and threat to ecosystems, the remediation of PFAS from the environment is crucial. Most conventional PFAS remediation methods for environmental matrices primarily focus on removing or stabilizing PFAS within the matrices. However, these methods are generally not able to completely degrade or destroy the compounds. Conventional techniques consist of sorption and chemical treatments. Additional disadvantages of these techniques include: 1) high cost, 2) adverse environmental effects, and 3) unsuitable for large-scale projects (Mahinroosta & Senevirathna, 2020). Conventional remediation techniques include: sorption to activated carbon, soil washing, and chemical oxidation.

A potentially cost-effective solution that does not negatively affect the environment and is suitable for large-scale projects is phytoremediation. "Phytoremediation is the use of plants and their associated microbes for environmental cleanup" (Pilon-Smits, 2005). The potential of phytoremediation was discussed by multiple studies showing that plants can be effective in the removal of PFAS (phytoextraction) from soil systems and surface waters (Gobelius et al., 2017; Kavusi et al., 2023; Mayakaduwage et al., 2022). However, studies on the potential of PFAS degradation by plants (phytodegradation) are limited.

This study aims to investigate whether perfluorooctanoic acid (PFOA) and perfluorooctanesulfonic acid (PFOS) can accumulate and subsequently be degraded in

plant tissues (leaves, stems, and roots) irradiated with UV light. The rationale for using UV light is to potentially activate ozonation in the plant tissues, particularly in the leaves. Ozonation increases the amount of oxygen radicals in the plant tissues, which may then induce PFOA and/or PFOS degradation (Trojanowicz et al., 2018). Of specific interest is the plant *Plantago major*, commonly known as (broadleaf) plantain ("grote weegbree" in Dutch). This plant species is selected based on its potential to accumulate high concentrations of PFAS, attributed to its high rates of evapotranspiration and biomass production. Plants are exposed to ^{13}C-labelled PFOA and PFOS to study bioaccumulation and potential UV-induced biodegradation. The natural abundance of stable carbon isotopes with a mass of 13 is approximately 1%. If PFOA and/or PFOS accumulate in the plants, their uptake will likely result in enhanced $^{13}C/^{12}C$ ratios in the plant tissues. Additionally, the $^{19}F/(^{12}C+^{13}C)$ ratio in the plant tissues will be used to detect PFOA and/or PFOS accumulation, since the natural abundance of Fluorine in plants is negligible. Elevated $^{19}F/(^{12}C+^{13}C)$ ratios in the tissues indicate PFAS accumulation. The $^{13}C/F$ ratio will serve as a proxy for potential UV-induced PFAS degradation. If PFAS degrades, fully or partially, one or more of the F atoms will separate from the ^{13}C atom. If the F atom is transported through the plant while the ^{13}C atom is "left behind", the $^{13}C/F$ ratio will increase in the areas where PFAS is localized within the plant tissue. Lastly, this study aims to assess the impact of UV light and/or PFAS exposure on the health *Plantago major* specimens.

Literature review

1. PFAS

1.1 PFAS classification

Although there is no universally accepted definition for PFAS, the OECD defines PFAS as follows: "PFASs are defined as fluorinated substances that contain at least one fully fluorinated methyl or methylene carbon atom (without any H/Cl/Br/I atom attached to it), i.e. with a few noted exceptions, any chemical with at least a perfluorinated methyl group (–CF3) or a perfluorinated methylene group (–CF2–) is a PFAS" (Wang et al., 2021). Another commonly used definition for PFAS is the following: "Perfluoroalkyl substances are defined as aliphatic substances for which all hydrogen (H) atoms attached to carbon (C) atoms have been replaced with fluorine (F) atoms, except for H atoms in the functional group" (Buck et al., 2011). An example of a perfluoroalkyl substance is perfluorooctanoic acid (PFOA; $C_7F_{15}COOH$) (fig. 1). 8:2 FTOH ($C_8F_{17}CH_2CH_2OH$), a fluorotelomer alcohol, is an example of a polyfluoroalkyl substance (fig. 1). Polyfluoroalkyl substances can relatively easily transform into perfluoroalkyl substances, since they contain C-H bonds which weaken the chain (Kavusi et al., 2023).

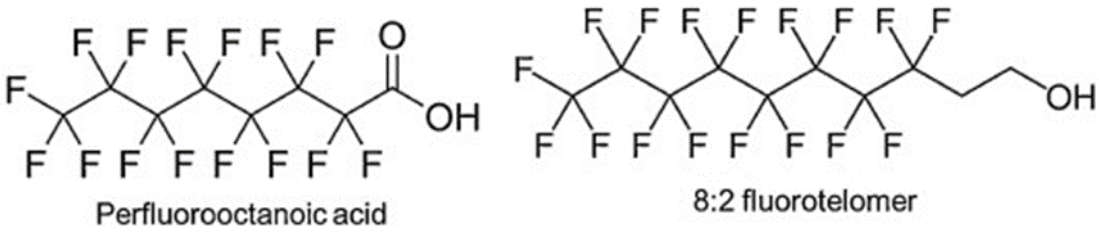

Figure 1: Chemical structures of perfluorooctanoic acid (PFOA) and 8:2 fluorotelomer (8:2 FTOH). (Adopted from Huang et al., 2023)

PFAS can be further classified by their polymeric form and by making distinctions between their functional groups (fig. 2). For example, PFOA is a perfluoroalkyl carboxylic acid (PFCA) and 8:2 FTOH is a fluorotelomer-based substance. The most common functional groups in PFAS are carboxylic or sulfonic acids (Kavusi et al., 2023). Both perfluoroalkyl carboxylic acids (PFCAs) and perfluoroalkane sulfonic acids (PFSAs) are called perfluoroalkyl acids (PFAAs).

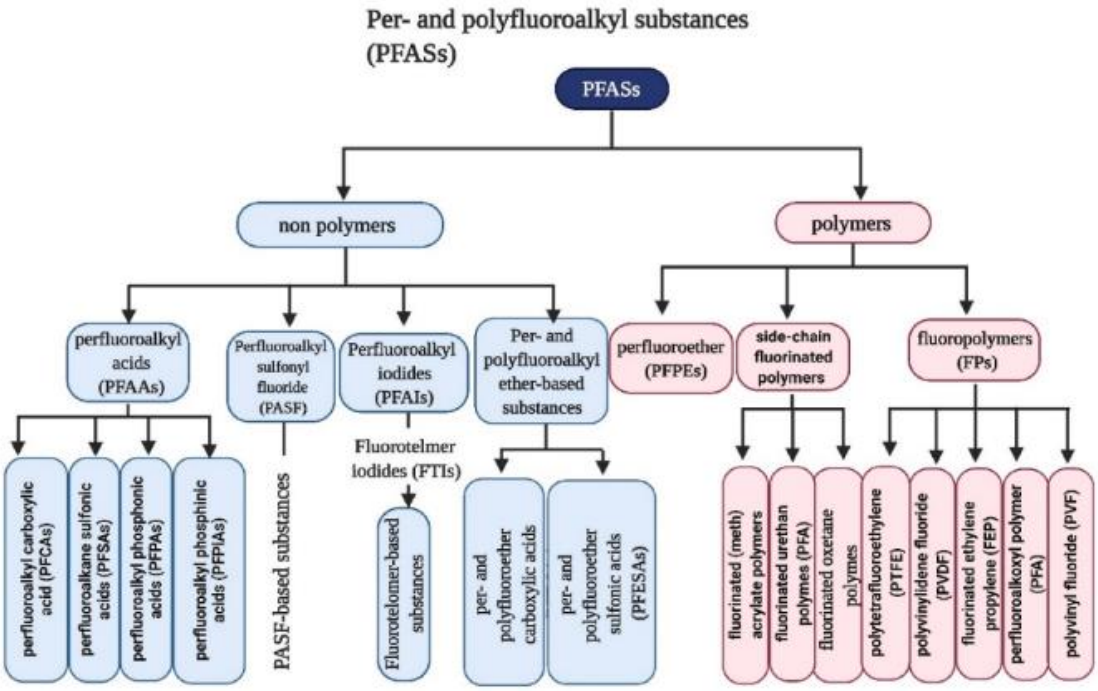

Figure 2: Further PFAS classification based on polymer form and functional groups. (Adopted from Kavusi et al., 2023)

Another common classification of PFAS used is by making a distinction between short-chain and long-chain groups. In the literature, no clear distinction between short- and long-chain PFAS is made. Ateia et al. (2019) distinguishes ultra-short-chain (C = 2-3), short-chain (C = 4-7) and long-chain PFAS (C>7) based on the total number of carbon atoms in the molecule. The two most common PFAS are PFOA and perfluorooctanesulfonic acid (PFOS), and both of these compounds are considered long-chain PFAS. A common ultra short-chain and short-chain PFAS are trifluoroacetic acid (TFA) and perfluorobutanoic acid (PFBA), respectively.

1.2 Physico-chemical properties of PFAS

The presence of fluorine gives PFAS unique properties when compared to their hydrocarbon analogues (Rice et al., 2021). Fluorine atoms are small and have a high electronegativity, which creates strong C-F bonds. The presence of extremely polar C-F bonds makes most PFAS exhibit (1) high chemical stability, (2) high thermal resistance, and (3) resistance to biotic degradation (Shahsavari et al., 2021). Additionally, the low polarizability of fluorine creates weak intermolecular

interaction and low surface energy, which gives PFAS both hydrophobic as well as lipophobic properties. The functional groups, on the other hand, are often highly hydrophilic, which gives PFAS both hydrophobic and hydrophilic properties (Rice et al., 2021). These properties make PFAS effective surfactants and surface protectors (Glüge et al., 2020). The length of the alkyl chain has a strong influence on the properties of the PFAS species. It was believed that short-chain (C<7) PFAS have a lower bioaccumulation potential and improved environmental properties in comparison to long-chain PFAS, but this is not necessarily the case. Both short-chain and long-chain PFAS are extremely persistent (Brendel et al., 2018). Short-chain PFAS have a shorter hydrophobic alkyl chain, which makes them more water soluble and less prone to adsorption and therefore more mobile in soil-water systems than long-chain PFAS.

1.3 The production of PFAS

The two most used methods for PFAS synthesis are electrochemical fluorination (ECF) and telomerization. During electrochemical fluorination, organic compounds are dissolved in anhydrous hydrogen fluoride. Subsequently, a direct current is passed through the solution, which results in the substitution of the hydrogen atoms of the organic compound with fluorine atoms (Dhore & Murthy, 2021). Telomerization is the most common technique for the production of the industrially relevant perfluoroalkyl acids (PFAA). Telomerization is generally a more expensive and complex approach compared to ECF, but the purity and the yield is higher (Dhore & Murthy, 2021).

1.4 The uses of PFAS

Due to their unique physico-chemical properties, PFAS are commonly used in a variety of industrial, commercial and consumer applications since at least the 1950's. A study from Glüge et al. (2020) identified more than 200 PFAS uses in 64 use categories for at least 1400 individual PFAS species. There are several use categories with more than 100 identified PFAS. These categories are "photographic industry", "semiconductor industry", "coatings, paints and varnishes", "firefighting foams", "medical utensils", "personal care products", and "printing" (Glüge et al., 2020). Well-known applications of PFAS include the use of PTFE (Teflon) as non-stick coatings in frying pans, PFAS-containing firefighting foams for extinguishing hydrocarbon fires, such as burning oils, fuels or alcohols, and the use of PFAS in (food) packaging to provide water and oil resistance (Gaines, 2023).

PFAS are, however, very costly to produce (100-1000 times more expensive than regular hydrocarbon surfactants) and are therefore specifically used when other substances cannot deliver the required performance or need much larger amounts to have the compared effect as PFAS (Glüge et al., 2020). Generally, PFAS are used for (1) processes or products that operate over a large temperature range, (2) processes or products that require stable and non-reactive substances , (3) products that require surface protection (PFAS used as surfactant) (Glüge et al., 2020).

2. PFAS contamination

2.1 Point Sources of PFAS

Since their introduction in the 1930's, PFAS have been entering environmental matrices through various pathways, primarily due to their widespread use for many applications in various industries. There are four major point sources of PFAS emissions, namely industrial facilities, firefighting foam usage, solid waste management facilities (landfills), and wastewater treatment plants (Meegoda et al., 2020).

2.1.1 Industrial facilities

Industrial facilities release PFAS to the environment by air emissions, release of incompletely treated wastewater effluents, accidental spills, and leakage. PFAS are released by industries as (a) primary products which include ingredients, residuals, and impurities, (b) as transformation products, or (c) as consumer goods containing PFAS (Dasu et al., 2022). Typically, PFAS concentrations in water and soil in the vicinity of fluorochemical manufacturers decrease with distance from the source, which confirms that the manufacturers are a major source of PFAS contamination in the environment (D'Ambro et al., 2021). For example, Figure 3 shows the spatial distribution of several PFAS species in the vicinity of a fluorochemical manufacturing facility in Fuxin, China (Chen et al., 2018).

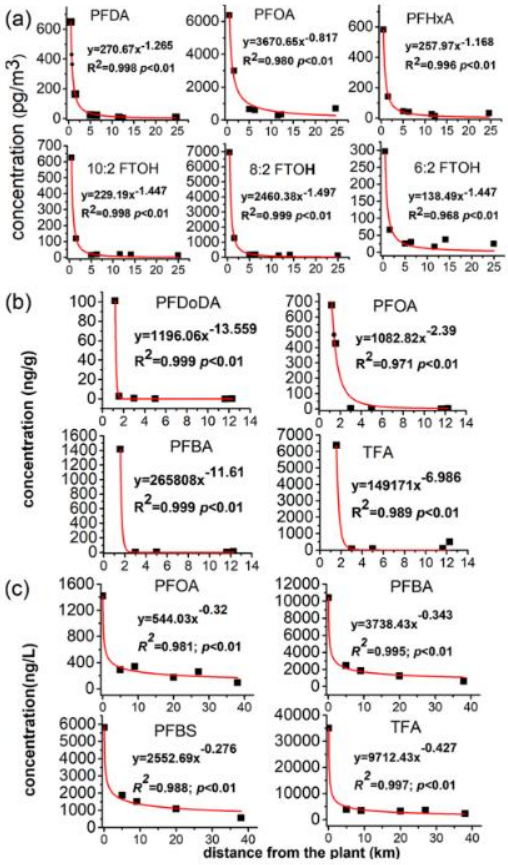

Figure 3: PFAS concentrations in (a) air, (b) outdoor settled dust, and (c) surface river water with distance from a fluorochemical manufacturer in Fuxin, China. (Adopted from Chen et al., 2018)

2.1.2. AFFFs

Aqueous Film-Forming Foams (AFFFs), which are a type of Class B firefighting foams, have been extensively used in high-risk areas prone to fire incidents, such as airfields and military training facilities (Meegoda et al., 2020). PFAS and hydrocarbon surfactants present in AFFFs reduce surface tension, which enables the foams to easily disperse over hydrocarbon fuel fires to extinguish the flames and prevent reignition (Dasu et al., 2022). Use of AFFFs leads to contamination of soils and waters in the vicinity of airfields and military training facilities, since many of these locations are not designed with AFFF containment (Milley et al., 2018). A 2019 study investigated a Norwegian firefighting training facility (FTF) and found PFAS concentrations ranging from <0.3 µg/kg to 6500 µg/kg in the soil at the FTF field site and found that PFOS accounted for 96% of the total PFAS concentration. The groundwater downstream from the site had an average PFOS concentration of 22 µg/L (6.5–44.4 µg/L), contributing to 71% of the total PFAS concentration (Σ 12-PFAS) (Høisæter et al., 2019).

2.1.3. Landfills

When PFAS- containing consumer goods are discarded, they likely end up in municipal solid waste management landfills. Following disposal, PFAS are released from the waste due to biological and abiotic processes and may afterwards leach into the environment. Leachate is the water that seeps through the disposed waste in landfills, carrying a mixture of harmful and persistent chemicals including pharmaceuticals and other environmental contaminants. The leachate is collected with liners for treatment at wastewater treatment plants (WWTPs). However, these WWTPs already contain PFAS from wastewater and are not able to (fully) remediate many PFAS species (Allred et al., 2015)(Hamid et al., 2018). PFAAs like PFCAs and PFSAs are the most commonly detected PFAS. The concentration of PFAS in landfills leachate varies greatly due to the heterogeneity of the waste that is disposed in the different landfills. A review of several studies found concentrations ranging from 0.03 µg/L to 292 µg/L in leachate (Stoiber et al., 2020). Additionally, landfills may also act as emission sources of atmospheric PFASs, as it was found that landfill ambient air contains elevated concentrations of PFAS in comparison to upwind control sites. This is probably due to the semi-volatile properties of several PFAS such as FTOHs (Hamid et al., 2018).

2.1.4. WWTPs

Wastewater treatment plants (WWTPs) are often considered as the most important point source of PFAS (Abunada et al., 2020). WWTPs receive PFAS enriched liquid waste from various sources, e.g. from municipal wastewater, leachate from landfills, and industrial wastes. As described above, wastewater treatment plants are not able to fully remove PFAS. A review study from 2020 compared several studies on PFAS concentrations and found that small, mobile PFAS concentrations in effluent (liquid that leaves WWTP) are significantly higher in comparison with influent (liquid that enters WWTP) (Stoiber et al., 2020). On the other hand, PFAS with longer-chains (C>9) decrease in the effluent compared to the influent. This is most likely caused by (bio)degradation of precursors into more stable shorter chain PFAS. The most commonly reported PFAS in effluents of WWTPs is PFOA with a median concentration of 255 ng/L and a maximum concentration of 15900 ng/L (Stoiber et al., 2020). The PFAS present in the effluents of WWTPs enters environmental matrices through direct discharge (surface and coastal water) or application of recycled wastewaters

(groundwaters, soils, and vegetation) (Lenka et al., 2021). Similar to landfills, WWTPs act as air emission sources of PFAS, mainly when treatments with aeration are occurring (Stoiber et al., 2020).

2.2 Environmental Fate of PFAS

PFAS are found in almost every region of the globe due to their widespread use (Panieri et al., 2022). Because of their diverse physico-chemical properties, the behaviour of PFAS in environmental matrices is complex (Meegoda et al., 2020). After being released to environmental matrices from point sources, PFAS can persist, transform, transport or accumulate in biota. Once PFAS are released from point sources into the environment, they can disperse and migrate through air, water and soil which leads to widespread distribution of the substances.

2.2.1 PFAS in the atmosphere

PFAS can enter and subsequently transport in the atmosphere via three mechanisms: volatilization, aerosolization and by particulate matter (Faust, 2023; Meegoda et al., 2020). Although most PFAS are less volatile compared to other organic contaminants, some species are still able to partition to the atmosphere (Panieri et al., 2022). Volatile PFAS species that have been detected in the atmosphere in gaseous phase include FTOHs, fluorosulfonamido alcohols (FSAs) and fluorotelomer acrylates (FTACs) (Meegoda et al., 2020). The approximate concentration range of these PFAS in the atmosphere generally is pg/m^3 (Panieri et al., 2022). PFCAs and PFSA, which are not particularly volatile, have also been detected in the atmosphere. These substances have high sorption potential and can adsorb to particulate matter, which facilitates their transport into the air. Field measurements show that partitioning from the gas phase to the particle phase becomes more favourable as the chain length increases and atmospheric temperature decreases (Faust, 2023). Additionally, wave breaking and bubble bursting processes in the sea can introduce PFAS to the atmosphere from the sea surface via sea spray aerosol particles (Faust, 2023). Volatilization, aerosolization and sorption to particulate matter, in combination with wind dispersion, all contribute to long-distance transport of PFAS. Atmospheric transport therefore leads to worldwide distribution of PFAS, even in remote places that are not affected by point sources. Atmospheric PFAS has been deposited as far afield as >400km from their source (Evich et al., 2022).

Although most PFAS that are released to the environment have high stability, about 20% of PFAS may undergo chemical transformation in the environment. This group of PFAS acts as precursors for stable or terminal transformation products, such as PFAAs. Precursors, like FTOHs or perfluorooctane sulfonamides, and fluorotelomer sulfonates, are common waste products of point sources (Prevedouros et al., 2006). Most volatile PFAS compounds tend to act as precursors for inert PFAS and atmospheric oxidation can lead to the formation of more stable PFCAs and PFSAs. This might be the reason that PFOA and PFOS are detected in Arctic snow. FTOHs and fluorosulfamido alcohols are transported to arctic regions and oxidize into PFOA and PFOS, respectively (Young et al., 2007). Atmospheric dispersion of PFAS has profound consequences in their subsequent transport towards other environmental matrices and their ecosystems (Panieri et al., 2022).

2.2.2. PFAS in surface water

There has been extensive research about the fate of PFAS in water, because waters are one of the main pathways of PFAS to human exposure (Abunada et al., 2020). Most PFAS are relatively soluble in water and are therefore commonly detected in surface waters such as lakes, rivers and even marine environments. PFAS can transport through surface waters in several ways. Firstly, PFAS in the dissolved phase can transport through surface waters by water flow (advection), dispersion and diffusion. Secondly, PFAS can transport through water as adsorped to suspended particulate matter. A study from 2010 found that within water, 97% of the PFAS was transported in the dissolved phase and only 3% by sorption onto suspended particulate matter. Short-chain PFAS (C<7) only transported as dissolved matter, PFAS with a chain length of 7>C>11 transported in the dissolved phase and on suspended particulate matter and long-chain PFAS C>11 were only found in the sediment (Ahrens et al., 2010)

The concentration range of PFAS in surface water has a large spatial variability, most likely due to presence of point sources in the vicinity of water bodies. For example, the total PFAS concentration (sum of 40 PFAS species) in the Rhine upstream of Leverkusen was found to be between 4.08-38.5 ng/L, while this concentration ranged from 119-268 ng/L downstream of Leverkusen. This dissimilarity is caused by an industrial WWTP in Leverkusen that acts as a point source of these compounds (Möller et al., 2010).

Seasonality also influences the PFAS concentrations. In the Asan Lake area in South Korea, the highest total PFAS concentrations (sum of 16 PFAS) were detected in Autumn and the lowest in the summer with concentrations of 270 ± 140 and 81 ± 29 ng/L, respectively. In South Korea, July and August are heavy rain periods, which probably dilutes the lake area, resulting in lower concentrations during the summer (Lee et al., 2020).

There are three sinks that can lower PFAS concentrations in surface waters, namely degradation, transport to deep ocean water and sediment burial. Similar to atmospheric oxidation, precursors of PFCAs and PFSAs, such as FTOHs may undergo chemical transformation in the water column. That being said, the PFCAs and PFSAs that form during this process remain highly persistent in aqueous environments and historical losses of these substances due to degradation are considered negligible. PFAS may be transported to deeper water due to downward flow or through sedimentation on sinking particles. The residence time of the PFAS in these deeper waters can be 300 to 500 years. Lastly, sediment burial refers to removal of PFAS below the bioturbated mixing layer that is available for exchange with the overlying water column (Prevedouros et al., 2006).

2.2.3 PFAS in soils

The fate and transport of PFAS in the soil are governed by processes that may either retain or remove them from soil. PFAS that reach soil can undergo sorption, partition and complexation, which causes them to be confined. In contrast, PFAS can be removed from soils by leaching, degradation/transformation, volatilization, and plant uptake (Bolan et al., 2021). The most dominant sources of PFAS contamination of soils are the release of AFFFs, atmospheric deposition, the use of contaminated water for irrigation and the application of biosolids or municipal sludge for agricultural practices (Panieri et al., 2022). After being released in soils, PFAS enter the vadose zone (unsaturated zone), and can subsequently flow downward to the phreatic zone (saturated zone). In the vadose zone, PFAS are retarded by two key processes, namely sorption to soil and accumulation at air-water interfaces. Because of their both hydrophobic and hydrophilic properties, PFAS are surface active which causes them to accumulate at air-water surfaces in the vadose zone (Sharifan et al., 2021). Sorption of PFAS to soil particles is caused by electrostatic interaction with charged clay and organic matter surfaces. Sorption of PFAS in soils increases with increasing chain-length of the PFAS and is also shown to increase with increasing organic matter

content (Bolan et al., 2021). Soil pH also influences PFAS sorption, as a decreasing pH of the soil increases the adsorption of PFAS compounds, likely due to increased positive charge because of H^+ dominance (Bolan et al., 2021). Sorption and air-water partitioning therefore increase the residence time of PFAS in the vadose zone. In soils with low sorption PFAS may leach in the phreatic zone (unsaturated zone) and can enter groundwater, which results in further distribution of PFAS in environmental matrices. Similar to PFAS in the atmosphere and surface waters, certain PFAS species may undergo transformation or volatilization. A comprehensive study from 2020 that measured worldwide PFAS concentrations in soils, revealed that PFAS were present in soil at almost every sampling location that was tested, even in remote regions far from potential PFAS sources. PFOA and PFOS were the most predominantly detected PFAS species. At PFAS contaminated sites soil concentrations ranged upwards of several hundreds of ppm. Generally, PFAS concentrations decrease with soil column depth, which indicates the dominance of the vadose zone of PFAS retention. The study clearly indicates, however, that PFAS have migrated to significant depths and also contaminate groundwater (Brusseau et al., 2020).

2.2.4 PFAS accumulation in plants

There have been numerous studies that show that PFAS can be taken up by plants and accumulate in their tissues (W. Wang et al., 2020) (Zhang et al., 2019) (Felizeter et al., 2012). Once PFAS permeate the vadose zone they become bioavailable to plants, which allows for their absorption through the roots. As discussed in "PFAS in soils", the primary sources of PFAS in the vadose zone are AFFF usage, atmospheric deposition and the use of PFAS contaminated water, biosolids and sludge for agricultural purposes. W. Wang et al. (2020) conducted a comprehensive review of multiple studies on plant uptake of PFAS, and summarized the main findings regarding PFAS uptake mechanisms in plants. Although, adsorption of PFAS particulates or uptake of gaseous PFAS via the shoots (green parts) of the plant can occur, the primary uptake pathway of PFAS in plants is through the roots. PFAS present in the vadose zone likely transports to plant roots due to the water potential gradient that is triggered by transpiration of the plants. It is unknown whether PFAS uptake in plants is an (energy-dependent) active or passive process. It is likely that a combination of both passive and active transport occurs, and that this varies among plant species and species of PFAS (Costello & Lee, 2020) (W. Wang et al., 2020). PFAS uptake by plants was found to be a concentration dependent process that could be well described by the Michaelis-

Menten model, which implies that the penetration of PFAS into the roots is likely carrier-mediated.

Following penetration through various root cellular structures, such as the epidermis, cortex, and endodermis, PFAS can enter the root vascular cylinder, allowing them to move upwards to the shoots of the plant (W. Wang et al., 2020). The translocation factor (TF) is a common indicator of the upward transport of PFAS in a plant species. The TF is the ratio of the PFAS concentration accumulated in the shoots and the concentration accumulated in the roots. The TF of PFCAs tends to decrease as the carbon chain length of the PFAS molecule increases, e.g., Perfluorobutanoic acid (PFBA) has a higher TF compared to PFOA. This phenomenon is also shown for PFSAs, but to a much lesser extent, indicating that PFSAs, such as PFOS, accumulate preferably in the roots of plants relative to PFCAs. (Adu et al., 2023). Another term that is frequently used to plant accumulation of contaminants is the bioconcentration factor (BCF) or bioaccumulation factor (BAF). This factor is defined as the ratio of the concentration of PFAS in the plant biomass to their concentration in the soil, and is used to determine the uptake potential of a plant species (Adu et al., 2023). The concentrations of accumulated PFAS in plants is typically in the range of µg/kg, but vary significantly among plant species. The extent of which PFAS are absorbed by plants depends on various factors, namely their concentration, chain length, functional group, plant species and variety, growth media, and soil and biosolid characteristics (Ghisi et al., 2018).

Physico-chemical properties of PFAS

In general, short-chain PFAS have a higher accumulation potential and TF in plants in comparison to long-chain PFAS. Short-chain PFAS are smaller in molecular size and have a higher solubility, which makes them less adsorptive to plant tissues and therefore more mobile than long-chain PFAS, which gives them a higher accumulation potential (Adu et al., 2023). Their lower adsorption also results in higher transferability within the plant when compared to long-chain homologues (Felizeter et al., 2012).

Plant physiological characteristics

The transpiration rate of a plant species plays a significant role in its uptake and transport of contaminants. Transpiration rate varies among plant species, plant structures, and even at different growth stages of a plant. Plant species with a higher transpiration rate contribute to a higher accumulation of PFAS (W. Wang et al., 2020).

In addition, it was found that vegetative structures (e.g., leaves and stem) tend to accumulate higher PFAS concentrations in comparison with storage structures (e.g., seeds), which is likely caused by enrichment from the transpiration stream (W. Wang et al., 2020). Furthermore, a positive correlation between PFAS enrichment and the plant mass was observed. The increasing biomass during plant growth offers more retention domains, enhancing the accumulation of PFAS. The protein and lipid content in plant roots also play a significant role in the plant root uptake of PFAS. The membrane bilayer primarily consists of lipids, while protein is associated with the abundance of transporters within the membrane. It is likely that protein content is positively correlated with the accumulation of PFAS in root tissues. On the other hand, the lipid content in roots seems to have a negative correlation with PFAS accumulation in the root tissues (Adu et al., 2023).

Surrounding environments

There are various surrounding environmental parameters that influence PFAS uptake by plants. The bioavailability of PFAS in soils to plants could be reduced due to soil sorption. Sorption of the soil generally increases with increasing soil organic matter and organic carbon content, and therefore PFAS uptake is inversely correlated with soil organic matter and carbon content. Additionally, increased soil organic matter and organic carbon content can enhance PFAS partitioning of PFAS in soils, which reduces PFAS in the dissolved phase, which means less PFAS is bioavailable (W. Wang et al., 2020). There are several other parameters that affect PFAS uptake, such as pH, temperature and salinity. As an example, increased temperatures can induce higher transpiration rates, which can lead to higher PFAS uptake.

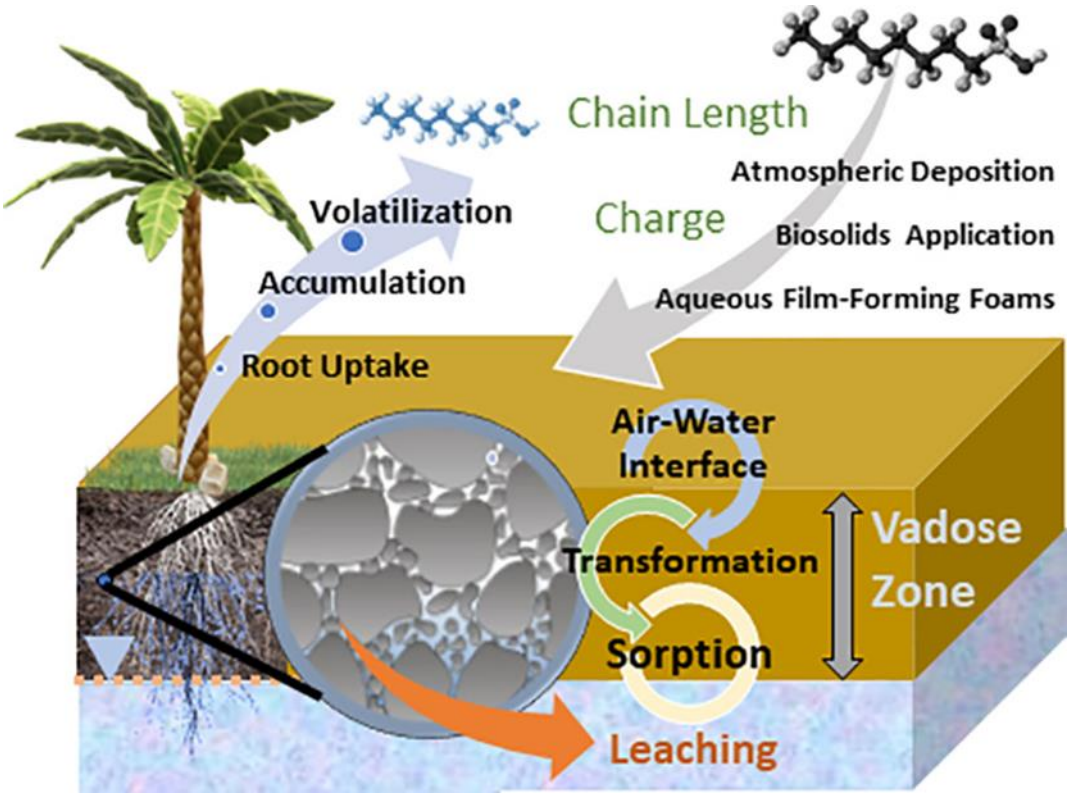

Figure 4: Graphical representation of the environmental fate of PFAS in soils and plants. (Adopted from Sharifan et al., 2021)

2.3 Impacts of PFAS on biota and human health

Following decades of widespread global use and because of their persistence and mobility, PFAS have raised concerns about the ecological and human health impacts (De Silva et al., 2021). Once present in environmental matrices, PFAS tend to bioaccumulate in both aquatic and terrestrial organisms. In the early 2000s, global concerns about potential health effects related to PFAS originated when PFOS was identified in the blood of polar bears in the Arctic and wildlife in other distant regions (Sunderland et al., 2018).

2.3.1 Impacts on Biota

PFAS tend to have a high binding affinity to serum albumin and fatty acid binding proteins. As a consequence, PFAS distribute within tissues of organisms in a manner that depends on the specific characteristics of these tissues (Ahrens & Bundschuh, 2014)

Aquatic ecosystems

There are multiple studies that show bioconcentration of PFAS in both freshwater and marine organisms (Gaballah et al., 2020; Haukås et al., 2007; Martin et al., 2003). Martin

et al. (2003) investigated the tissue distribution and bioconcentration of PFCAs in rainbow trout and found that PFCA concentrations were highest in the blood and lowest in the muscle tissue of the fishes. Interestingly, short-chain PFAS (C<7) were not detected in most tissues, and the bioconcentration significantly increased with increasing chain length for PFAS with a chain length between 8 and 12 carbons. The study does not comprehensively discuss the toxicological effects of PFAS on the fish, but a mortality rate of 2% (one fish) was found for the exposed group in comparison with 0% in the control group, which is probably a random death. The growth of the fish during the experiment was similar between the control group and the exposed group. Haukås et al. (2007) reports the concentration and biomagnification potential of PFAS in species from the Barents sea food web and found no correlation between PFOS concentrations and trophic level within species. Out of the PFAS that were tested (PFOS, PFOA, PFNA, PFHxS, PFHxA, PFDcA, and 6:2 FTS) PFOS displayed the highest bioconcentrations in the different species, with a maximum concentration of 225 ng/g found in liver tissue of Glaucous gulls. Gaballah et al. (2020) assessed the potential toxicity of several PFAS (e.g. PFOA, PFOS, PFHxA, and PFHxS) on zebrafish, and found that the potencies of the PFAS were correlated with increasing carbon chain length concerning neurotoxicity, though this correlation was not observed for developmental toxicity.

Terrestrial ecosystems

Although there are numerous studies that investigated bioaccumulation in aquatic species, much less is known about bioaccumulation in terrestrial organisms. Most studies are focused on plants. A comprehensive study by Gredelj et al. (2020), observed inhibited growth, discolouration of leaves and visible root damage of hydroponically grown chicory plants when exposed to high (125 and 250 µg/L) PFAA concentrations. However, these physiological changes of the plant did not affect the plant's bioaccumulation efficiency (Gredelj et al., 2020). Zhao et al. (2011) aimed to derive soil toxicity values (NOEC, EC_{10}, EC_{50}) for PFOS and PFOA in *Brassica chinensis* and found high values in the range of mg/kg soil. However, the findings indicated that soil properties could play a role in influencing the plant's response to the toxicity of PFOA and PFOS (Zhao et al., 2011). Apart from plants, there are also multiple studies on bioconcentration in earthworms, since they are an important source of prey for small mammals and birds (Nazmul Ehsan et al., 2024). Navarro et al. (2016) found PFAS concentrations ranging from 9.9 to 101 ng/g in earthworms that lived in soils exposed

to biosolids containing 20 PFAS (Navarro et al., 2016). Health effects were not considered.

2.3.2 Impacts on human health

Sunderland et al. (2018) conducted a comprehensive review of PFAS and human health, covering both the pathways of human exposure and the associated health effects. Their findings will be summarised in this section.

Human exposure pathways

PFAS exposure to humans occurs through consumption of contaminated drinking water and seafood, inhalation of indoor air, and coming into contact with other contaminated substances. PFAS are widely used in various consumer products (e.g., jackets, upholstery, carpets, and papers) and can therefore come in direct contact with humans. Furthermore, PFAS can migrate from food packaging to consumables, which poses another direct exposure route to humans. Ultimately, it is believed that food is the main exposure pathway of PFAS in humans. Precursors of PFAS in consumer products can transform into PFAS in the human body, and inhalation of volatile precursors is also known to occur (Sunderland et al., 2018). For numerous populations, drinking water has also been identified to be a significant source of PFAS exposure. In the USA, PFOA was detected in 59% of the public water supplies and the maximum concentration amounted to 190 ng/L. High concentrations of PFAS in drinking water are often found in water supplies in the vicinity of point sources. Estimating the total PFAS concentration in drinking water becomes more challenging, because of the introduction of newer PFAS, such as GenX (Sunderland et al., 2018). Sadia et al. (2023) aimed to investigate the occurrence of PFAS in drinking water in the Netherlands at 18 different locations. Their research found that in all drinking waters, trifluoroacetic acid (TFA), PFBA, and PFOA were present. PFOS and PFHxA were also found in the majority of drinking waters. Ultrashort-chain PFAS (e.g. TFA) were found to have the highest concentrations (300-1100 ng/L), followed by PFCAs (0.4 to 95.1 ng/L). Drinking waters that are produced from surface water tend to have higher total PFAS concentrations compared to drinking water that is produced from groundwater (Sadia et al., 2023). It is reported that several populations with high consumption of seafood, such as Inuit men in Greenland, whaling men in the Faroe Islands, and commercial fishery employees in China, have elevated serum concentrations of PFAS. PFAS concentrations in seafood are generally higher next to contaminated sites. The extent

to which seafood contributes to the overall exposure of humans to PFAS varies significantly. According to the European Food Safety Authority (EFSA), fish and other seafood is responsible for as much as 86% of dietary PFAS exposure in adults (Sunderland et al., 2018). The last major pathway for human exposure to PFAS is the use of biosolids as fertilizers in agriculture, which leads to elevated PFAS concentrations in crops and farm animals (Sunderland et al., 2018).

Human health effects

The 3M Company has conducted multiple studies on the health effects of PFAS exposure in animals and humans since the 1990s, as they played a significant role to human exposure as a primary global manufacturer of PFAS. Although these studies remained mostly unpublished for years, eventually they revealed the acute animal toxicity of PFAS and unveiled elevated serum PFAS concentrations in 3M workers. Subsequent animal studies on rats, mice, and monkeys showed adverse health effects, including cancer and toxicity on the immune system. PFOA exposure was found to cause potential alterations in male reproductive hormones and leukocyte counts (Sunderland et al., 2018).

In the early 2000s, the amount of conducted academic studies started to increase, due to the phase-out of PFOS and its precursors. Numerous studies have investigated the carcinogenicity of PFAS, but are mainly focused on PFOA and PFOS. PFOA and PFOS have been associated with increased risk of prostate cancer mortality, kidney and testicular cancer. That being said, there are multiple studies that did not find an association between plasma PFOA and PFOS concentrations and cancer. PFAS are also studied with regards to their potential immunotoxicity, and particularly children seem to be at risk. Outcomes of these studies include both molecular-level outcomes, such as decreased antibodies, or organ/system-level outcomes, e.g., infections to the respiratory system. Studies that investigated the association between PFAS exposure and the suppression of antibody response to vaccination found potential immunosuppression due to PFAS. In contrast, results on organ/system level are more inconsistent. Slightly more than half of the studies investigating the influence of PFAS on asthma and infections show significant results, but these studies have their limitations. PFAS can however have a substantial effect on metabolic processes in the human body. The strongest evidence for a link between PFAS exposure and metabolic changes is with regards to dyslipidaemia, which are imbalances of lipids such as

cholesterols and triglycerides. There are indications that PFAS might interfere with neurodevelopmental effects, but neurodevelopmental trajectories are complicated due to heterogeneity in the instruments and methods used during studies. It is therefore necessary to conduct additional research to establish a relationship between neurodevelopmental outcomes and PFAS exposure (Sunderland et al., 2018).

2.4 Conventional soil remediation techniques for PFAS

The remediation of PFAS from contaminated solid and aqueous is very complicated, since PFAS (1) exhibit high chemical and thermal stability, (2) are often found in complex mixtures in contaminated media, (3) have unique physico-chemical properties, and (4) are extremely persistent (Bolan et al., 2021). Soil remediation can be divided into three categories: sorption, destruction technologies, and separation technologies (Mahinroosta & Senevirathna, 2020).

2.4.1 Sorption

This technique involves the redistribution of PFAS from the solution to the solid phase, consequently reducing their mobility and bioavailability (Bolan et al., 2021). Sorbents are added and subsequently mixed with contaminated soils to reduce PFAS leaching from the vadose zone to the groundwater. A variety of sorbents have been tested in laboratories as well as in the field, including activated carbon (AC), resins, minerals, and polymers (Mahinroosta & Senevirathna, 2020). Generally, activated carbons are the most used sorbents and granular activated carbon (GAC) has been shown to consistently remove PFOS with an efficiency of over 90% (Kucharzyk et al., 2017). Nevertheless, the adsorption conductivity of AC is highly variable depending on factors such as the type of AC (e.g., powdered AC (PAC) or GAC), the specific PFAS variant (short-chain vs long-chain), and the properties of the contaminated soil (pH, soil organic matter content, etc.) (Gagliano et al., 2020). Thermal incineration is a common practice for treating spent activated carbon. Typically thermal incineration of PFAS requires temperatures of over 1000°C, but laboratory studies indicate that 99% of PFOS can be removed at temperatures of around 600°C. Degradation temperatures of PFAS tend to increase with longer chain lengths (Kucharzyk et al., 2017).

Despite demonstrating excellent PFAS removal efficiencies, adsorption technologies are burdened by high operation and maintenance costs, along with the need for frequent regeneration of the sorbent (Mayakaduwage et al., 2022).

2.4.2 Destruction of PFAS

During destruction technologies, PFAS is completely degraded in the soil, mostly by using chemical treatments and biological remediation.

Chemical treatments

In chemical oxidation, an oxidant is introduced to react with a contaminant and transforms it into non-toxic, degradable byproducts (Mayakaduwage et al., 2022). In general, PFOA and PFOS degradation was found to be ineffective using common chemical oxidative/disinfection methods, such as chlorination, ozonation and chemical oxidation. However, during certain conditions chemical treatments can still be effective in the removal of PFAS from soils. There are several studies that utilized in-situ chemical oxidation (ISCO) with persulfates and were able to degrade PFOA to concentrations below the detection limit (Bolan et al., 2021). Chemical treatments, while effective, are unsuitable for large-scale soil remediation projects. The use of certain chemicals can be expensive and can lead to environmental concerns (Bolan et al., 2021).

Bioremediation

Although most PFAS are likely barely biodegradable, investigations have inferred that limited biotransformation of PFAS can occur (Shahsavari et al., 2021). This biotransformation mostly brakes down precursors into more stable PFAS. There are studies that have attempted biodegrade PFOA and PFOS using microbes, but no effective method has been found and further investigation is necessary (Mayakaduwage et al., 2022). Research on fungal degradation of PFAS also suggests potential PFOA and PFOS degradation, but again further research is needed to confirm this.

2.4.3 Separation technologies

Separation technologies detach contaminants from the soil or sediment in which they persist. The most common separation technology in the removal of PFAS is soil washing (Mahinroosta & Senevirathna, 2020). During soil washing, soil is excavated and

washed with an extracting agent, such as water. Due to the high solubility of PFAS, soil washing detaches adsorped PFAS from the soil. A pilot-scale study conducted in Sweden treated 10 tonnes of soil using soil washing, achieved 96% separation of PFOS from soil particles. After these results a large-scale project was conducted aiming to treat 1500 tonnes of contaminated soil. The results were promising as the PFOS concentration in washed soil reduced to 17 μg/kg (Initial concentration ~425 μg/kg and remediation goal was 29 μg/kg). However, the project had some drawbacks as only 10% of the anticipated 1500 tonnes of contaminated soil was actually treated (Bolan et al., 2021). Other disadvantages of soil washing are that excavation projects of soil can be very costly, particularly in clayey soils. Moreover, the process generates polluted water that requires additional treatment (Kavusi et al., 2023).

3. Phytoremediation

"Phytoremediation is the use of plants and their associated microbes for environmental cleanup" (Pilon-Smits, 2005). The technology utilizes natural processes within plants and their microbial rhizosphere to degrade and sequester both organic and inorganic pollutants (Pilon-Smits, 2005).

3.1 Mechanisms of phytoremediation

The mechanisms and efficiency of phytoremediation depend on the type of pollutant, the properties of the soil, and the bioavailability of the pollutant (Etim & Etim, 2012). Plant employ various mechanisms to clean up and remediate contaminated sites, namely phytostabilization, phytoextraction, phytostimulation, phytodegradation, and phytovolatilization (Pilon-Smits, 2005).

3.1.1 Phytostabilization

Phytostabilization is a form of phytoremediation, by which plants are used to stabilize contaminants in the soil, either by preventing erosion, leaching, or runoff, or by transforming contaminants into less bioavailable compounds (Pilon-Smits, 2005). This technique is mostly used for the immobilization of heavy metals on contaminated sites, such as mine tailings (Mendez & Maier, 2008). Plants have the ability to effectively immobilize heavy metals in soils through sorption to their roots, precipitation, complexation or metal valence reduction in the rhizosphere. However, phytostabilization is not a permanent solution, because contaminants are simply stabilized and not removed from the soil (Ali et al., 2013).

3.1.2 Phytoextraction

Phytoextraction is the uptake of contaminants from environmental media by plant roots (Ali et al., 2013). Plants can accumulate contaminants in their roots or their shoots. With this remediation technique, contaminant accumulation in the shoots of the plant is preferred, since these plant tissues are easiest to harvest, while root removal from soils can be challenging (Ali et al., 2013). The harvested material can subsequently be used for non-food purposes, recycled in the case of valuable contaminants (phytomining) or incinerated (ashed), followed by disposal in landfills (Pilon-Smits, 2005).

3.1.3 Phytostimulation

Plants can promote biodegradation of pollutants by microbes in their rhizosphere. This remediation technique is called phytostimulation, commonly known as rhizodegradation. This technique is commonly used for the remediation of hydrophobic organic pollutants that cannot accumulate in the tissues of the plant, but can be degraded by microbes, such as polychlorinated biphenyls (PCBs) and polycyclic aromatic hydrocarbons (PAHs) (Pilon-Smits, 2005). The primary reason for enhanced contaminant degradation in the rhizosphere is likely the increased abundance and metabolic activity of microbes. Plants can boost the microbial activity in the rhizosphere by up to 10-100 times through the excretion of carbohydrates, amino acids, and flavonoids, which the microbes use as carbon and nitrogen sources. Additionally, plants secrete enzymes that can aid in contaminant degradation (Ali et al., 2013).

3.1.4 Phytodegradation

Degradation of compounds can also occur within the organs of a plant using their own enzymatic activities. This phytoremediation technique works well for organic compounds that have a high mobility in plants, such as trichloroethylene (TCE), Methyl tert-butyl ether (MTBE), or perhaps PFAS (Pilon-Smits, 2005). Complex organic pollutants are transformed within the plant into simpler compounds that the plant may use for its growth (Khan et al., 2023).

3.1.5 Phytovolatilization

During phytovolatilization, accumulated pollutants are volatilized in the plant into their gaseous phase. Phytovolatilization can be used as a treatment technology in the remediation of sites contaminated with organic compounds and several heavy metals, such as mercury and selenium (Ali et al., 2013). A plant species with a high transpiration (e.g. poplar trees) rate is favoured for this remediation technique (Pilon-Smits, 2005).

3.2 PFAS phytoremediation

This paragraph reviews the potential of phytoremediation of PFAS by sharing the outcomes of various studies on the subject of PFAS uptake by plants.

3.2.1 Translocation and bioaccumulation of PFAS in three wetland species

Awad et al. (2022) studied the translocation and bioaccumulation of long-chain PFAS compounds (PFOA and PFOS) in three wetland plant species (*Phragmites australis, Baumea articulata and Juncus krausii*). They found that the shoot uptake of both PFOA and PFOS increased as the exposure time increased. Furthermore, increasing the PFOA/PFOS exposure concentrations also lead to increased shoot uptake. For all three plant species, PFOS accumulated at significantly higher concentrations in the roots than PFOA, while PFOA accumulated in the shoots at significantly higher concentrations than PFOS. Translocation of PFOA from the roots to the shoots was therefore more effective compared to the translocation of PFOS. The uptake efficiency of PFOA and PFOS was most dominant in *Phragmites australis* (mean: 53% and 42% respectively), followed by *Baumea articulata* (29% and 24%) and then *Juncus krausii* (5% and 5%). These findings suggest that certain plant species offer a potential extraction method in the removal of PFAS from surface water. CFW (constructed floating wetland) systems can be planted with species such as *Phragmites australis* and extract long-chain PFAS from surface waters. Subsequently, plants can be harvested from the CFW systems and replanted regularly (Awad et al., 2022).

3.2.2 Phytoremediation potential of various plant species

Gobelius et al. (2017) investigated the PFAS uptake of several plant species (*Betula pendula, Picea abies, Prunus padus, Sorbus aucuparia, Aegopodium podagraria, Phegopteris connectilis, and Fragraria vesca*). To do this, the researchers collected samples of twigs and foliage of these plant species in the vicinity of a contaminated fire training facility and analyzed the concentrations of a total of 26 PFAS. Ten out of the 26 PFAS were found in plants. The highest total PFAS concentrations were found in foliage of birch (*Betula pendula*), spruce (*Picea abies*), and bird cherry (*Prunus padus*). For the twigs the most dominant species were again birch, spruce, and bird cherry. However, the total PFAS concentration in the twigs of all species was significantly lower compared to the foliage, although falling within the same order of magnitude. Based on these findings, the authors also discuss the potential of phytoremediation of these plant species. They proposed three management scenarios in which phytoextraction is used to remove PFAS from the contaminated sites, and claim that phytoremediation of PFAS is a very cost-effective, passive, sustainable and low maintenance technique. That being said, phytoremediation is a slow, long-term approach.

3.2.3 Possible phytodegradation

There is a limited number of studies that investigate the potential of phytodegradation of PFAS. To my knowledge, there are only two recent studies by Greger & Landberg (2024), and Guo et al. (2022) that investigated potential PFAS transformation in plants. Although not the main aim of their study, one of the research questions of Greger & Landberg (2024) was to investigate whether certain enzymes (laccases and peroxidases) are involved in plants' removal and degradation of PFAS. Laccases and peroxidases are produced in plants and used in several processes in plants. Enzymes were added to the nutrient solutions (which contained PFAS) of growing plants, and subsequently the enzyme activities and concentrations were measured at various timepoints. The results showed that 24h presence of laccases degraded PFOS and PFBA by 5% and that peroxidases degraded PFHxA and PFHxS by 2% (Greger & Landberg, 2024). Guo et al. (2022) aimed to understand the impacts of dissolved organic matter in soil on the absorption and transformation of 6:2 chlorinated polyfluoroalkyl ether sulfonate (6:2 Cl-PFESA) in wheat (Triticum aestivum L.). Recent investigations suggest that 6:2-PFESA has potential to transform into 6:2 hydrogen-substituted polyfluorooctane ether sulfonate (6:2 H-PFESA) in rainbow trout and rats. Guo et al. (2022) found that dissolved organic matter (DOM), such as fulvic acid, and humic acid, promoted transformation of 6:2 Cl-PFESA in wheat (Guo et al., 2022).

3.3 Advantages and limitations of phytoremediation

Phytoremediation has garnered increasing scientific interest due to its competitive performance, environmentally sustainability, and cost-effectiveness (Mayakaduwage et al., 2022). However, phytoremediation techniques also have their drawbacks. Both advantages and limitations of phytoremediation will be outlined in this section.

3.3.1 Advantages of phytoremediation

An important reason for the use of phytoremediation is the cost-effectiveness of the technique. Currently, costs associated with environmental remediation are extraordinary. Approximately $25-50 billion per year is spent worldwide on environmental remediation (Pilon-Smits, 2005). The process of phytoremediation is fuelled by the sun, which makes the technique a tenfold cheaper than conventional engineering-based remediation techniques such as excavation (Pilon-Smits, 2005). Phytoremediation is also a mainly passive process, which means that the maintenance

of a phytoremediation project is low (Gobelius et al., 2017). Additionally, phytoremediation is environmentally friendly. Conventional remediation methods may endanger ecosystems, due to the use of harsh chemicals and invasive excavation. Phytoremediation, on the other hand, relies on the natural processes of plants to remediate contaminated sites (Kavusi et al., 2023). Moreover, the biomass that is generated during the treatment can be utilized for various purposes, such as the production of biogas and fuel wood, and to recover the contaminants back from the plant tissues (Mayakaduwage et al., 2022).

3.3.2 Limitations of phytoremediation

There are many limitations that might make phytoremediation not a feasible option for the removal of contaminants from environmental matrices. Most of the research on phytoremediation is carried out in a controlled situations within short time trials. This might not be representative in field conditions for a long time period. More field trials have to be conducted based on a longer time period to figure out the true potential of phytoremediation (Kafle et al., 2022). Additionally, consumption of contaminated plant tissues by animals poses a contamination risk of food chains. This can also lead to an exposure pathway to humans in cases where plants may be edible (Mayakaduwage et al., 2022). Another limitation is that phytoremediation will likely not work in severely contaminated sites, since the highly concentrated contaminants at these sites drastically affect the health of the plants. Sometimes resistant non-native plant species that are resistant to certain pollutants may be introduced to ecosystems and can have negative effects on the species within that ecosystem. Furthermore, the technique is dependent on the depth distribution of the roots of a plant species, and may only be able to extract contaminants from shallow water or soil depth (Mayakaduwage et al., 2022). Seasonality is also a limitation since during the winter months plant growth is moderate or even ceased.

Methods

1. Chemicals

The PFAS used in this study were isotopically labelled ^{13}C PFOA (purity >99%) and ^{13}C PFOS (purity > 99%). These chemicals were purchased from Wellington Laboratories (Canada). Hoagland Basal Salt mixture, purchased from Sigma-Aldrich, was used as the fertilizer for the plants throughout the study. This mixture contains essential elements for plant growth and is free of fluorine-containing substances.

2. Plant collection and preparation treatments

2.1 Plant Collection

Adult specimens of *Plantago major* were collected from three different local parks in the Netherlands: one in Utrecht, one in Nieuwegein, and one near Gouda. Plants were dug out carefully from the soil using a garden hand trowel and it was made sure that the roots of the harvested plants were undamaged. In addition to the plants collected from outside, plants were grown from seeds obtained from Cruydt-Hoeck (Cruydt-Hoeck, Nijeberkoop, the Netherlands). These seeds were germinated and grown in a greenhouse using potting soil as growth medium.

2.2 Preparation treatments

After collecting the plants, they were carefully but thoroughly rinsed with tap water, followed by three washings with deionized water to remove soil from the surface of the roots and shoots of the plants. The plants were then transferred into 84-ml polypropylene (PP) plant pots. Polystyrene disks (1 cm thickness) were cut with a diameter of 5 cm and placed in the plant pots to support and stabilize the plants. A hole (r= 0.5 cm) was drilled into the polystyrene disk and the plant pot through which the roots of the plants were placed. The plants were grown using a hydroponic system i.e., no soil was used. The pots containing the plants were subsequently transferred into 212-ml glass jars filled with 80 ml of half-strength Hoagland solution, ensuring that only the roots of the plants and the glass jars were in direct contact with the solution (image 1). This setup was designed to maximize the bioavailability of both the nutrients and the PFAS that would be added to the solutions during the exposure

experiments. Glass jars were chosen based on a study from 2022 that investigated PFAS adsorption to containers and found that glass generally adsorbs less PFOA and PFOS to its surface compared to plastics (Zenobio et al., 2022). An additional purpose of the polystyrene disks in the plant pots was to inhibit evaporation of water from the glass jar. Prior to exposure with PFOA or PFOS, the plants were given at least two weeks to acclimatize to their environment, which enabled recovery of the plants that were potentially damaged during collection. If both root and shoot growth was observed during the acclimatization period, plants were assumed to be healthy enough for the experiments with PFAS exposure.

Imag

3. Experimental Design

The study focused on bioaccumulation and degradation of PFOA and PFOS in the plant species *Plantago major*.

3.1 Growing environment

Plants were grown for a maximum duration of 28 days within two separate fume hoods in a laboratory, with a temperature between 18 and 25°C. The motive for conducting the experiments in fume hoods was for safety reasons regarding human health. One fume hood was designated for experiments with UV-light, while the other was designated for experiments without UV-light. To prevent cross-contamination of UV-

light, the two fume hoods were completely isolated. In both fume hoods a white full spectrum growing light (2500 lumen, Hornbach) with a 12h light/12 h dark cycle was placed above the plant samples at a height of approximately 40 cm. In the fume hood with UV exposure (+UV), two UV lamps with 30% UV-A and 12% UV-B (300 lumen, Monkfield Reptile, Ely UK) were placed at a similar height above the plants. The UV lights that were used in this study simulate the sun in a desert environment.

3.2 Exposure experiments

After the acclimatization period, the nutrient solutions of the plants were replenished to their original volumes. For the samples that were to be exposed to PFAS, either ^{13}C-labelled PFOA or ^{13}C-labelled PFOS was added to their nutrient solutions. Additionally, several plants did not receive PFAS treatments and served as controls. Right after replenishment, mass measurements were performed as described in the section "Growth of *Plantago major*". Plants were randomly placed within the respective fume hoods. The study was split into three experiments that were carried out simultaneously.

The first experiment aimed to investigate whether PFOA and/or PFOS are able to accumulate in *Plantago major* under hydroponic conditions. Both fume hoods (+/- UV light) were used for this experiment. Plants were exposed to a concentration of 25 µg/L of ^{13}C labelled PFOA or PFOS. This concentration was applied because comparable studies used PFAS concentrations of the same order of magnitude (µg/L) (Awad et al., 2022; Gredelj et al., 2020; He et al., 2023; Zhang et al., 2019; Zhang & Liang, 2020). Each treatment had two or three replicate plant to assess biological variability and to cover for potential plant decay in certain samples during the growing period. Plants were harvested after 3, 7, 14 and 28 days, washed with deionized water, and subsequently stored at -20°C before further EA-IRMS analysis and NanoSIMS analysis. Control plants that did not receive PFAS treatment were harvested on the same timepoints as plants that were exposed to PFAS. To assess for the natural ^{13}C/^{12}C ratio in *Plantago major* two plant samples were harvested immediately after the acclimatization period. These plants were never exposed to ^{13}C-labelled PFAS.

The second experiment aimed to investigate whether there is a correlation between the initial PFAS concentration in the Hoagland solution and the amount of PFAS that accumulates in the plant. A total of four plants were exposed to a lower concentration (2.5 µg/L) of ^{13}C labelled PFOA or PFOS. Two of these plants were grown under UV-

light (+UV), while the remaining two were grown in the other fume hood (-UV). All four plants were harvested after 28 days, washed with deionized, and stored at -20°C before further EA-IRMS analysis.

The third experiment aimed to investigate whether *Plantago major* can degrade PFOA and/or PFOS when the plant is irradiated with UV-light. Plants were grown in both fume hoods and exposed with 25 μg/L ^{13}C-labelled PFOA or PFOS and were harvested after 28 days. After harvesting the plants were washed with deionized water and the plants were stored at -20°C before further sample preparation for NanoSIMS analysis. Control plants that were used in the first experiment were also used for this experiment to compare exposed and non-exposed samples.

During the study period the plants were replenished with Hoagland solution when needed.

4. Growth of *Plantago major*

In addition to the experiments with regards to PFAS uptake and degradation, the influence of PFAS and UV light on the growth of *Plantago major* was determined. To monitor the growth, the masses of the glass jar, the nutrient solution, the plant (including the pot), and the combined mass are determined at the beginning of the study period.

In practice, this process was performed as follows: first the combined mass of the glass jar and the solution was determined by lifting the plant pot with the plant out of the glass jar. Subsequently, the plant pot and plant were placed back into the jar, and the total mass was measured. The difference between this total mass and the mass of the glass jar + solution, can be assumed to be the mass of the plant pot + plant at the start of the experiment.

After 7, 14, 21 and 28 days, the masses of the jars, nutrient solution, plant pots and the plants were determined. The mass of the glass jars and the plant pots did not change throughout the study period, so the initial mass of the plant is equal to the difference between the mass of the plant pot + pot at the beginning of the experiment and the mass of the plant pot at the end of the experiment. The mass difference between the final mass and the initial mass of the plants is equal to the net biomass gain of the plant samples.

This mass experiment is carried out for all control plants and plants that were exposed to PFAS with a concentration of 25 μg/L (i.e., excluding the plant exposed to concentrations of 2.5 μg/L). To assess possible mass changes in the glass jars and the plant pots, empty glass jars and plant pots were randomly placed in the fume hood among the plants, and their mass was measured every 7 days.

5. Bulk analysis

Elemental Analyser Isotope Ratio Mass Spectrometry (EA-IRMS) was used to determine whether the plants had accumulated PFOA or PFOS during the study period. After freezing, plants received another washing with deionized water and were separated into plants that were analyzed with EA-IRMS and plants that were analyzed with NanoSIMS. The plants were separated into the following plant tissues: roots, leaves, and stems. Plant tissues that were analyzed with EA-IRMS initially underwent a freeze drying period of 24 hours. Freeze dried material was homogenized using a mortar and a vessel and stored in 10 mL Greiner tubes at room temperature. Following the homogenization of each plant tissue, the laboratory utensils (i.e., mortar, vessel, laboratory spatula) were washed with 96% ethanol, followed by drying using tissue wipes. Approximately 0.6 mg of dried material was weighed and placed in tin capsules for EA-IRMS analyzation. In addition to the experimental samples, positive controls were prepared to verify whether the chemicals were in fact ^{13}C labelled and to see whether EA-IRMS was feasible for analyzing PFAS concentrations in plant tissue. To create these controls, approximately 0.6 mg of dried material from the t=0 plants was placed in a tin capsule. Then, 100 μL of a stock solution containing 0.6 mg/L of ^{13}C-labelled PFOA/PFOS was added to the tin capsule. This was done for three replicates of both PFOA and PFOS. The tin capsules were subsequently oven-dried at 50°C to remove any methanol and water present in the PFAS solution. The theoretical increase in $\delta^{13}C$ of these positive controls is described in text box 1 on page 38.

The EA-IRMS results provide the $\delta\ ^{13}C$ (‰) and the mass fraction of carbon relative to the total mass $C_{fraction}$ (%) in the plant tissues.

The following equations are taken form a 2017 study that investigated the behavior of phenanthrene in soil-plant systems by adding ^{13}C labelled phenanthrene. The study utilized EA-IRMS to measure the $\delta^{13}C$ values in the soil and plants within these

systems. These measurements served as a proxy to track and understand the dynamics of phenanthrene within the soil-plant systems (mesocosms) (Cennerazzo et al., 2017).

Isotopic measurements were reported in the delta ^{13}C notation (in ‰), which is expressed in equation 1.

$$\delta 13C\ (‰) = \left(\left(\frac{R_{sample}}{R_{ref}}\right) - 1\right) \text{x } 1000 \qquad (1)$$

Where $R_{sample} = {}^{13}C_{sample} / {}^{12}C_{sample}$ for labelled samples, and R_{ref} is equivalent to the Vienna Peedee Belemnite (VPDB) standard, which is equal to 0.01118. R_{sample} was determined from the EA- IRMS results using equation 2.

$$R_{sample} = \left(\left(\frac{\delta 13C}{1000}\right) + 1\right) \text{x } R_{ref} \qquad (2)$$

The enrichment in ^{13}C (E_{13C}), which is expressed as excess % of atoms was calculated relative to the unspiked controls using equation 3.

$$E_{13C} = (13C_{labelled} - 13C_{control}) \qquad (3)$$

Where $13C_{labelled}$ and $13C_{control}$ can be calculated using equations 4 and 5 respectively.

$$13C_{labelled}\ (\%) = \left(\frac{R_{labelled}}{(R_{labelled} + 1)}\right) \text{x } 100 \qquad (4)$$

$$13C_{control}\ (\%) = \left(\frac{R_{control}}{(R_{control} + 1)}\right) \text{x } 100 \qquad (5)$$

Subsequently, the ^{13}C concentrations ($13C_{conc}$) expressed as µg C g^{-1} in the different plant tissues were calculated using equation 6.

$$13C_{conc}\ (\mu g\ C\ g^{-1}) = \left(\frac{(13C_{labelled} - 13C_{control})}{100}\right) \text{x } C_{fraction} \qquad (6)$$

Where $C_{fraction}$ refers to the carbon content, expressed in µg C g^{-1} of the dried plant tissue.

The translocation factor (TF) was also calculated for both PFOS and PFOA using equation 7.

$$TF = \frac{13C_{conc,leaves} + 13C_{conc,stems}}{2 \text{ x } 13C_{conc,roots}} \qquad (7)$$

Where $13C_{conc,\ tissue}$ (μg C g^{-1}) denotes the ^{13}C concentration in the respective plant tissue.

Theoretical $\delta^{13}C$ increase in the positive controls:

100 µL of 0.6 mg/L PFOA or PFOS was added to tin capsules along with 0.6 mg of dried leaf material. The dried plant material consists of approximately 40% carbon, meaning that each capsule contains 0.24 mg or 19.9817 µmol derived from the plant tissues (C_{nat}). Assuming that the abundance of that the abundance of ^{13}C relative to ^{12}C in the plant tissues is equal to the VDPB standard (=0.01118), the amount of ^{13}C ($13C_{nat}$), expressed in µmol, that is naturally present in the plant tissues can be calculated using equations S1

$$R_{nat} = \frac{13C_{nat}}{12C_{nat}} = 0.01118 \qquad (S1)$$

Where $12C_{nat}$ represents the amount of ^{12}C in the sample, expressed in µmol. The amount of ^{12}C in the sample can be assumed to be equal to C_{nat} - $13C_{nat}$. Substituting this into equation S1 yields equation S2.

$$\frac{13C_{nat}}{C_{nat} - 13C_{nat}} = 0.01118 \qquad (S2)$$

Solving for $13C_{nat}$ yields the following equation:

$$13C_{nat}\ (\mu mol) = \frac{0.01118\ x\ C_{nat}}{1 + 0.01118} \qquad (S3)$$

The ^{13}C mass fractions ($13C_{m,frac}$) in both ^{13}C-labeled PFOA and PFOS were calculated using equation S4.

$$13C_{m,frac,PFAS} = \frac{(n_C * MN_{13C})}{MW_{PFAS}} \qquad (S4)$$

Where n_c is equal to amount of carbon atoms in the respective PFAS molecule (8 for both PFOA and PFOS), MN_{13C} stands for the mass number of ^{13}C (=13), and the MW_{PFAS} denotes the molar weight of the respective PFAS (PFOA = 422, PFOS = 508). This fraction allows for the calculation of the amount of ^{13}C in the PFAS molecules ($13C_{PFAS}$), expressed in µmol, by using equation S5.

$$13C_{PFAS}\ (\mu mol) = \frac{13C_{m,frac,PFAS}\ x\ V_{added}\ x\ PFAS_{conc}}{MN_{13C}} \qquad (S5)$$

With V_{added} equal to the volume of the stock solution added to the tin capsules, expressed as µL (=100), and $PFAS_{conc}$ representing the PFAS concentration of the stock solution (=0.0006), expressed in µg/µL. The addition of this PFAS solution raises the $^{13}C/^{12}C$ ratio of the sample (R_{sample}). The new ratios for PFOA and PFOS are expressed by equation S6:

$$R_{sample} = \frac{13C_{nat} + 13C_{PFAS}}{12C_{nat}} \qquad (S6)$$

Equation S6 is valid under the condition that all methanol present in the stock solution evaporates during the oven-drying step. Utilizing equation S6, the following ratios are found for the positive controls of PFOA and PFOS, respectively: 0.01124 and 0.01123.

Equation S7 provides theoretical $\delta^{13}C$ values of +5.37‰ and +4.47‰ for the positive controls of PFOA and PFOS, respectively.

$$\delta 13C\ (‰) = \left(\left(\frac{R_{sample}}{R_{ref}}\right) - 1\right) \text{x } 1000 \qquad (S7)$$

Text box 1: Theoretical $\delta^{13}C$ estimation of positive control samples.

6. NanoSIMS analysis

Nanoscale secondary ion mass spectrometry (NanoSIMS 50L Cameca, Paris France) was used to determine the spatial distribution of accumulated PFAS in the plant tissues and to investigate whether PFAS degradation occurred in the plants.

The sample preparation protocol for plant tissues to make them suitable for NanoSIMS analysis was developed in collaboration with section Cell Biology from the University Medical Center Utrecht (UMC Utrecht). Because of their extensive experience with different methods for chemical fixation, embedding, and sectioning using microtomes, the sample preparation for NanoSIMS analysis of *Plantago major* was fully conducted at the laboratory facilities of the section Cell Biology.

Due to the time-intensive process of the sample preparation, a selection of six plants was made. All of these plants were grown for 28 days. The selected plants include:

1. UV treated plant, exposed to PFOA
2. UV treated plant, exposed to PFOS
3. UV treated plant, not exposed to PFAS
4. Plant not treated with UV, exposed to PFOA
5. Plant not treated with UV, exposed to PFOS
6. Plant not treated with UV, not exposed to PFAS

After freezing, plants that were to be analyzed with NanoSIMS were washed with deionized water. Next, small sections of the different plant tissues (leaves: 5x5 mm, stems: 5mm x width of stem, and roots: 1 cm x width of root) were cut using a razor blade. To ensure no cross-contamination occurred between plant-tissues, the razor

blade and cutting board were consistently washed with deionized water. After cutting, sections were chemically fixated for at least 24 hours using Karnovsky fixative. After fixation, the tissues were rinsed with deionized water and were dehydrated using graded series of acetone (50%, 70%, 90%, 95%, and 100%) incubations. The first dehydration steps lasted one hour each at 50%, 70%, 90%, and 95%, while the 100% dehydration step was carried out overnight. Dehydrated materials were then embedded in a graded series of EpoFix (Agar Scientific, Essex UK). The plant tissue was incubated in each solution (25%, 50%, 75%, and 100% resin with acetone) for at least one hour during the initial (25%, 50%, 75%) incubation steps, and overnight for the final 100% incubation step. The resin was then cured for 24 hours at room temperature (21°C). After curing, 200 nm sections were cut using a microtome (Leica Microsystems, Wetzlar Germany). The sections were mounted on silicon wafers (7 x 7 mm) and left to dry. Prior to NanoSIMS analysis, the samples were coated with 10 nm gold to ensure a conductive sample surface.

Scanning Electron Microscopy was utilized to verify the suitability of the prepared samples for NanoSIMS analysis, to spatially identify areas with well-preserved cell structures, and to determine the anatomical structure of the plant tissues in the samples.

High resolution maps of the plant tissues were acquired using a NanoSIMS 50L. Cs^+ primary ion beam was used to examine the sections of the plant tissues. The following negative secondary isotopes were detected: $^{12}C^-$, $^{13}C^-$, $^{12}C^{14}N^-$, $^{19}F^-$, $^{31}P^-$, and $^{32}S^-$. The mass spectrometer was optimized using an aperture and an energy slit and set to a mass resolution of at least 6000 to distinguish between ^{13}C and ^{12}CH. Firstly, pre-sputtering of areas of interest (~80 μm^2) was performed for approximately 20 minutes using a beam current of 200 pA and an impact energy of 16 keV. Afterwards sputtering of a smaller areas (~40 μm^2) was performed using beam currents of ~1-2 pA. Images were acquired with a dwell time of 1 ms per pixel and 256 x 256 pixels. NanoSIMS data analysis was performed as previously described by Polerecky et al. (2012).

To verify the presence of organic plant material in the samples and to distinguish between plant material and resin, combined $^{12}C^{14}N^-$, $^{31}P^-$, and $^{32}S^-$ images were generated. Subsequently, regions of interest (ROIs) were identified and classified as edges, organelles, and resin using the spatial distribution of the organic matter and the resin. Images of the $^{13}C/^{12}C$ ratio were generated to detect possible PFAS accumulation

in the tissues. In addition, images of the $^{19}F/(^{12}C+^{13}C)$ ratio were generated as another proxy for PFAS accumulation. To detect possible PFAS degradation, images of the $^{13}C/F$ ratio were generated.

7. Data visualization and statistical analysis

The results were collected and visually represented using Excel, while R was employed for the statistical analysis of the data. Linear mixed modelling was utilized to evaluate the effect of UV light and PFAS exposure on the growth of *Plantago major*. Additionally, this modelling approach was used to evaluate the correlation between $\delta^{13}C$ values measured in the different plant tissues and PFAS exposure to the plants. A hypothesis was considered to be statistically significant when the p value was lower than 0.05.

Results

1. Growth of *Plantago major*

This section assesses the impact of both UV-light and PFOA/PFOS on the growth of *Plantago major*.

1.1 Visual assessment and fungi

Throughout the duration of the study, the majority of the plants maintained a healthy appearance and did not seem to suffer because of UV light and PFAS exposure. No significant differences in morphology and color was observed between growing plants subjected to UV-light and plants that were not subjected to UV light. In addition, plants that were treated with PFAS did not notably differ in morphology or discoloration compared to controls. All the plants exhibited growth of existing leaves and the emergence of new leaves. However, it is important to note that a fungus was detected on a large number of the plants. Fungi were present in both fume hoods and affected plants regardless of the treatments. Individual leaves showed discoloration, ultimately leading to desiccation of the leaf.

1.2 Net biomass

Figure 5a illustrates the net biomass gain of plants that were subjected to UV treatment, while figure 5b displays the net biomass gain of plants that did not undergo UV treatment. Note that each data point in Figure 5 represents the net biomass gain of an individual plant; for example, a plant harvested and weighed on day 7 was not weighed again on days 14 or 28. After the study period, there was a significant variability in the net biomass gain of the plants. Surprisingly, a great amount of plants showed a decrease in biomass. Overall, the mean final plant mass was larger than the mean initial plant mass, with average increases of 0.144 g for plants that received UV treatment and 0.104 g for plants that did not receive UV treatment. However, no significant correlations were found between the net biomass gain and the day of harvest for either treatment ($p=0.095$ and $p=0.196$). Additionally, the net biomass gain of plants did not show any correlation with the various PFAS exposure treatments in both +UV and -UV treatments(PFOA: $p=0.226$ and $p=0.389$, PFOS: $p=0.197$ and $p=0.976$, respectively).

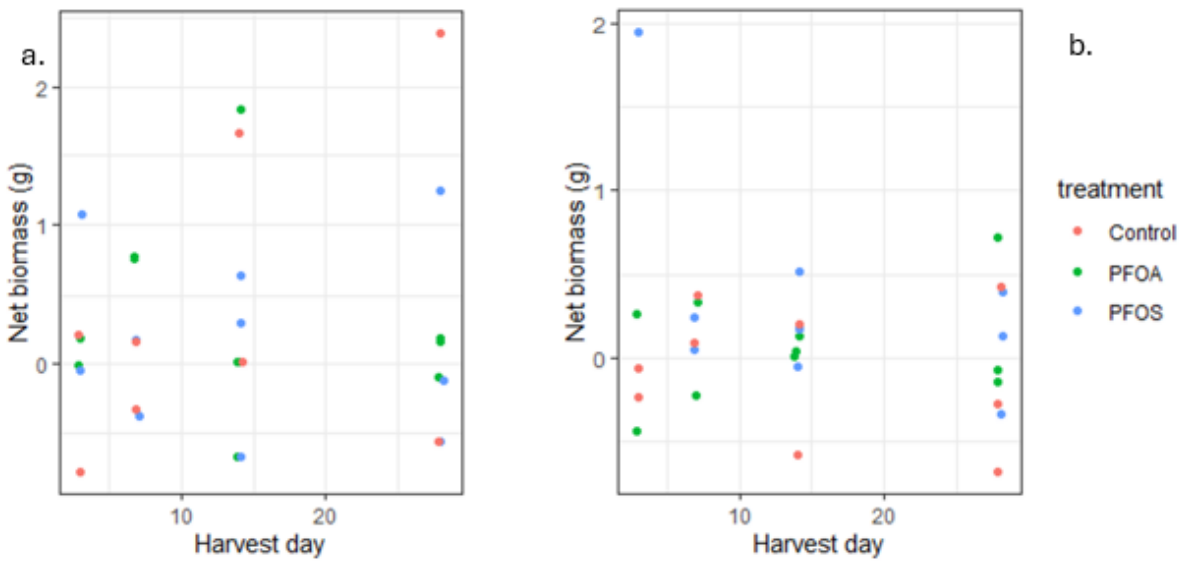

Figure 5: Net biomass of the plants that were subjected to UV light (a) and the plants that were not subjected to UV light (b).

Figure 6a and 6b display the initial masses of the plants plotted against the net biomass gain for both the treatments with UV exposure and without UV exposure, respectively. The analysis was conducted to investigate whether a higher initial weight of a plant would favor its net biomass gain. For the +UV treatment the initial weight of the plants correlated significantly with net biomass gain at the harvest day of the plant (p=0.001), indicating that a higher initial biomass of a plant led to greater biomass production during the study period. However, this correlation was not observed for the plants that did not receive UV treatment (p=0.848).

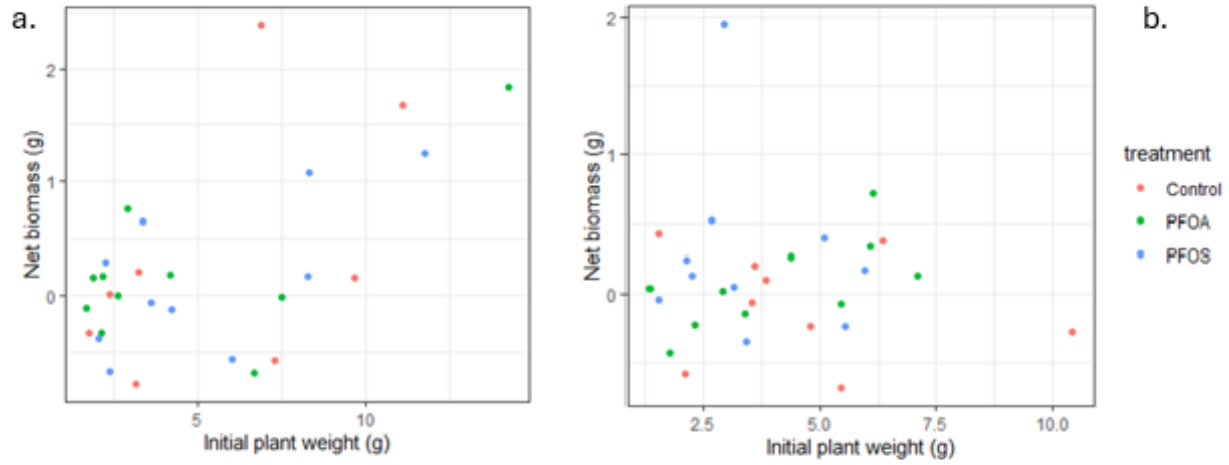

Figure 6: The initial mass (weight) of the plants at the start of the study period plotted against their net biomass gain for plants that were subjected to UV light (a) and plants that were not subjected to UV light (b).

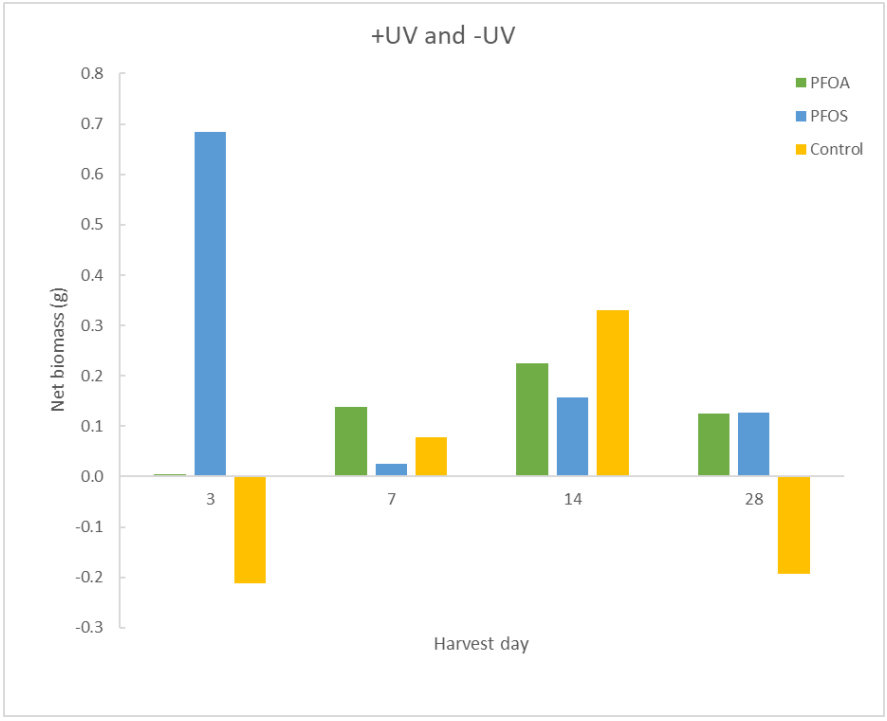

Figure 7: The mean net biomass gain of plants exposed to PFAS and controls regardless of light treatment.

For visualization, figure 7 illustrates the mean net biomass gain of plants exposed to PFAS compared to the controls regardless of light treatment. Notably, the plants that are exposed to PFOS have the highest mean net biomass gain, followed by PFOA and finally the control group, with mean values of 0.248, 0.123 and 0.000, respectively.

However, it is important to note that these mean values may not be statistically significant and could be attributed to chance.

2. Bulk Analysis

This section examines the findings with regards to the uptake of PFOA and/or PFOS by *Plantago major*.

2.1 Plant carbon content & $\delta^{13}C$ values

The mean carbon content fluctuated among the different plant tissues, yet remained unaffected by UV or PFAS treatments. Specifically, the average carbon content for leaves, stems, and roots were 38.69% (34.04-41.25%), 36.93% (31.55-39.71) , and 40.03% (35.72-43.10%, respectively.

Delta ^{13}C ($\delta^{13}C$) values are summarized in table 1 and figure 8 for plants that were subjected to UV-light. There was a lot of $\delta^{13}C$ variability among the samples, which makes detecting PFAS incorporation in the plants impossible. The mean $\delta^{13}C$ values for plants that have been exposed to PFOA, PFOS, and no PFAS (controls) are -30.22, -29.74, and -29.93, respectively.

UV Treatment

		$\delta^{13}C$ (‰)		
Harvest day	*Plant tissue*	PFOA	PFOS	Control
t= 0 days	Leaves	X	X	-32.36
	Stems	X	X	-31.90
	Roots	X	X	-31.48
t= 7 days	Leaves	-31.44	-31.02	-28.71
	Stems	-30.60	-30.25	-28.65
	Roots	-30.00	-30.34	-28.20
t= 14 days	Leaves	-29.01	-30.26	-29.81
	Stems	-28.30	-29.74	-29.04
	Roots	-28.03	-28.86	-28.73
t= 28 days	Leaves	-32.19	-30.40	-31.31
	Stems	-31.42	-28.82	-30.10
	Roots	-30.98	-27.99	-28.92
Positive control	Leaves	-25.94	-29.85	X

Table 1: $\delta^{13}C$ values for plants that received UV treatment.

No UV Treatment

		$\delta^{13}C$ (‰)		
Harvest day	*Plant tissue*	PFOA	PFOS	Control
t= 0 days	Leaves	X	X	-32.36
	Stems	X	X	-31.90
	Roots	X	X	-31.48
t= 7 days	Leaves	-28.44	-29.62	-27.22
	Stems	-28.31	-29.07	-27.17
	Roots	-28.48	-28.81	-27.18
t= 14 days	Leaves	-28.03	-30.25	-33.99
	Stems	-27.83	-29.42	-33.14
	Roots	-27.61	-29.61	-33.01
t= 28 days	Leaves	-29.78	-31.35	-29.98
	Stems	-28.25	-29.79	-27.59
	Roots	-28.00	-29.30	-28.00
Positive control	Leaves	-25.94	-29.85	x

Table 2: $\delta^{13}C$ values for plants that did not receive UV treatment.

Table 2 and figure 9 summarize $\delta^{13}C$ values for plant that were not subjected to UV-light. Again no significant relationships between the PFAS treatments and the $\delta^{13}C$ values were found. The mean $\delta^{13}C$ values for plants that have been exposed to PFOA, PFOS, and no PFAS (controls) are: -28.30, -29.69, and -30.25. By utilizing the controls as a reference, the natural $^{13}C/^{12}C$ ratio for *Plantago major* in this trial was determined to be 0.01084 using equation 1.

For the positive controls, mean $\delta^{13}C$ values were found to be -25.94 for PFOA and -29.85 for PFOS. The mean $\delta^{13}C$ value found for the positive controls with PFOA aligns with the theoretical expectation described in text box 1. However, the alignment is less clear for the positive controls with PFOS. Although the mean $\delta^{13}C$ for PFOS is higher compared to the leaves of the plants that were harvested at t=0 (-29.85 vs. -32.36), the expected increase should have been around +4.47‰.

For visualization, $\delta^{13}C$ values for all the individual samples that were analyzed using EA-IRMS are summarized in figure 8 for the UV treatment and figure 9 for the -UV treatment.

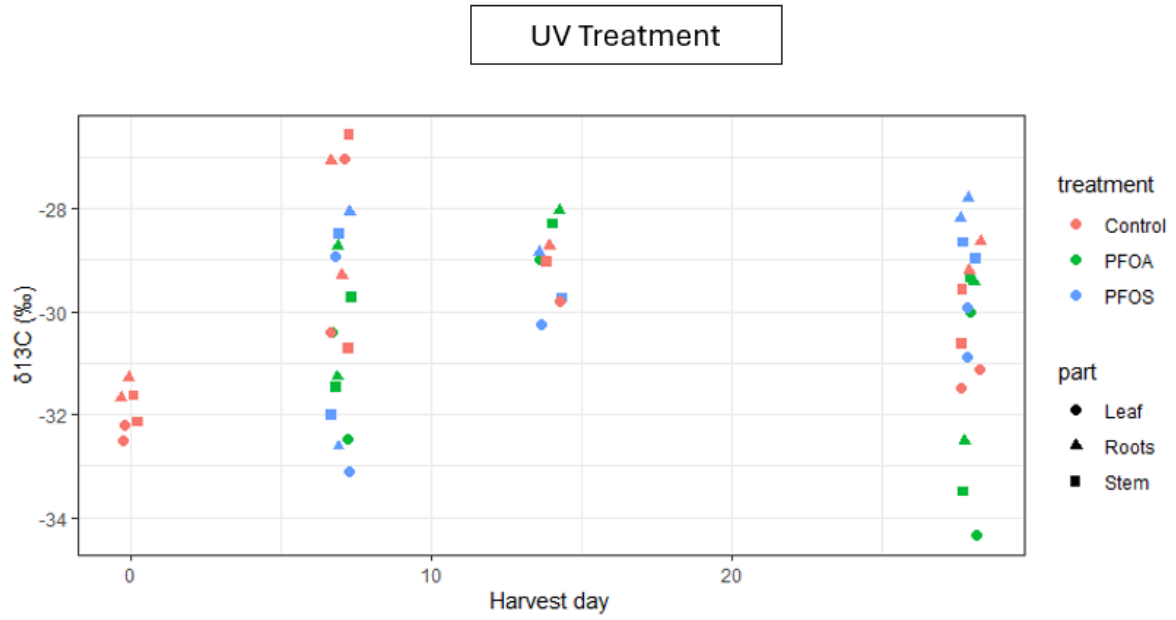

Figure 8: Visualization of $\delta^{13}C$ values for plants that received UV treatment.

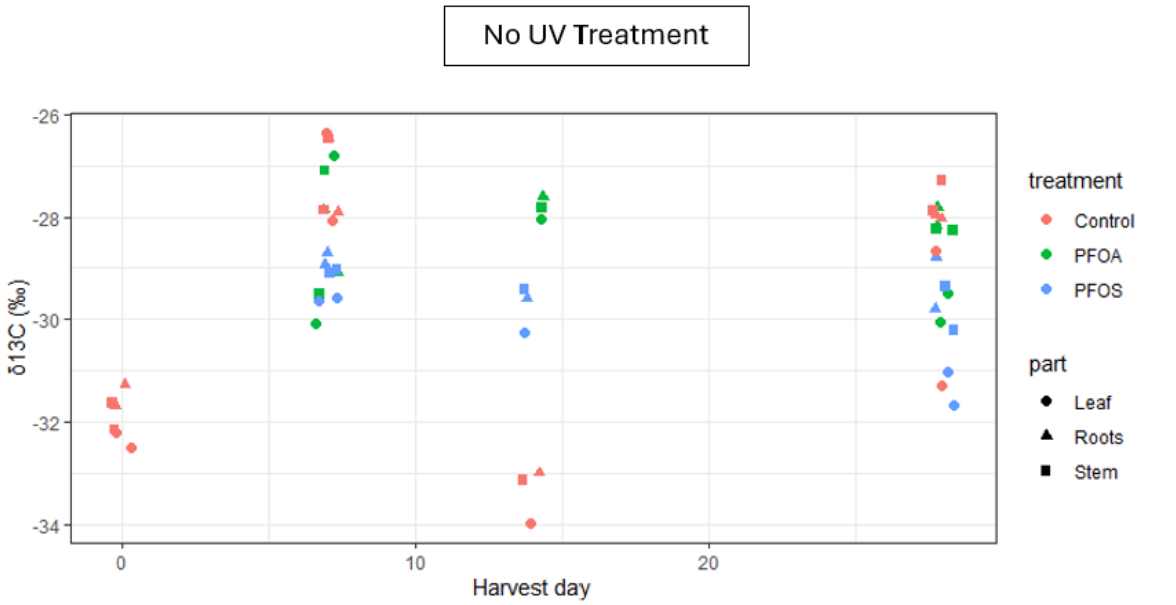

Figure 9: Visualization of $\delta^{13}C$ values for plants that did not receive UV treatment.

2.2 Further calculations

Because the biological variance of the $^{13}C/^{12}C$ ratio among different plants exceeded the expected increases attributed to the presence of PFAS, it was impossible to determine whether accumulation of PFAS in the plant tissues had occurred. This led to insignificant further calculations of the accumulated PFAS concentrations in the tissues and the translocation factors.

3. NanoSIMS analysis

This section presents the findings of the NanoSIMS analysis, specifically addressing the spatial distribution of accumulated PFAS and the findings with regards to potential PFAS degradation.

3.1 Analyzed samples

Out of the eighteen prepared samples, six were suitable for NanoSIMS analysis. Most of these samples include embedded leaves, with only one sample being from the roots. Due to the fact that only one sample of a root was suitable, it was excluded from further NanoSIMS analysis. Table 3 summarizes the samples that were analyzed. The leaf that was exposed to PFOA and did not receive a UV treatment, was analyzed at three distinct locations within the leaf.

UV Treatment	*PFAS Treatment*	*Plant tissue*
No UV	PFOA	Leaf
No UV	PFOS	Leaf
No UV	Control	Leaf
UV	PFOA	Leaf
UV	PFOS	Leaf

Table 3: Samples of plant tissues that were analyzed with NanoSIMS.

Three samples exhibited notably elevated $^{13}C/^{12}C$ ratios in certain locations within the sample. These samples will be discussed, while the remaining samples that did not show clear elevated $^{13}C/^{12}C$ ratios will be included in the appendix.

3.2 Preservation of the plant tissues

SEM images of the samples are visualized in figure 10. Despite the damage to the cell structures of the plant tissues occurring during the sample preparation, sufficiently well-preserved areas of the plant were detectable and suitable for analysis. The green boxes represent the areas of the samples that were analyzed with NanoSIMS.

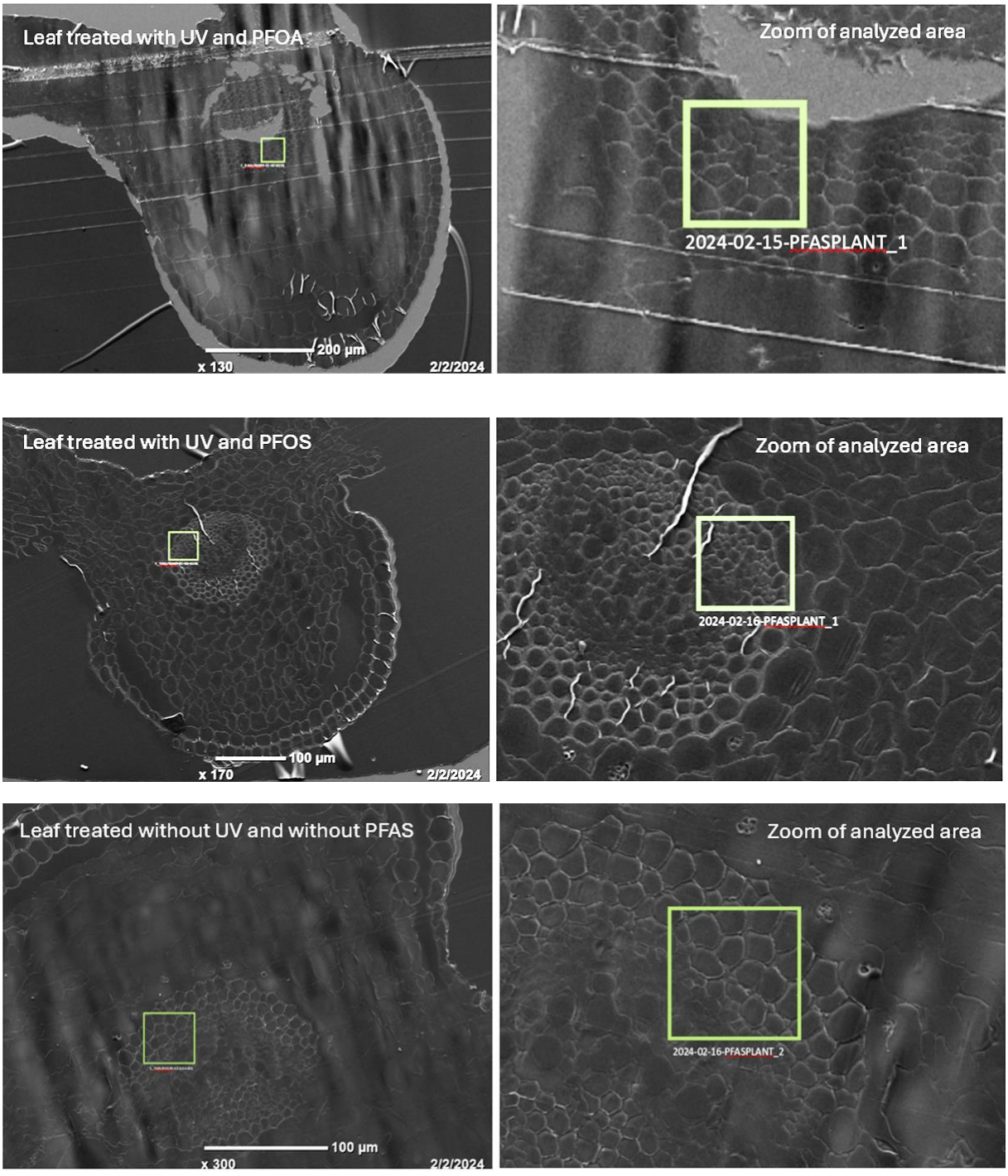

Figure 10: SEM images of the analyzed leaf samples.

Comparing the SEM images from this study to microscopic images from a 2017 study by Mesquita et al. (fig. 11) allows for the identification of the anatomical structure of Plantago major leaves and verification of the preservation of these structures during the sample preparation. The leaf treated with UV and PFOS is used for comparison, as its cross-sectional morphology most closely resembles the microscopic image from Mesquita et al. (2017).

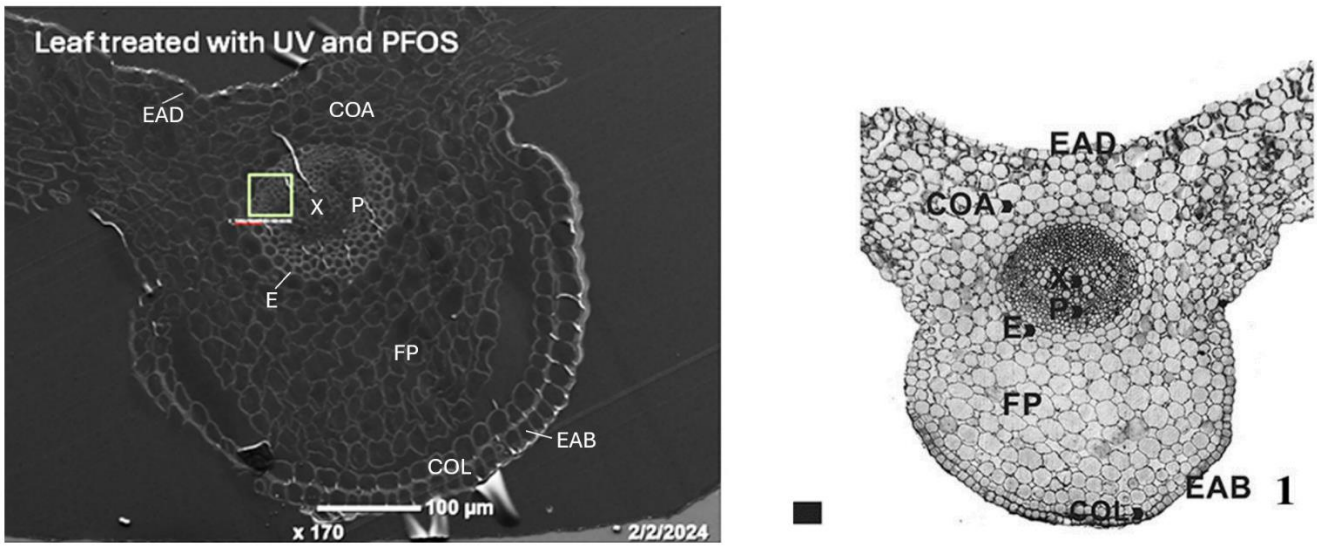

Figure 11: Left: SEM image from this study of a *Plantago major* leaf treated with UV and PFOS with anatomical features. Right: Microscopic image of a cross section of a *Plantago major* leaf, adopted from Mesquita et al. (2017) used for comparison. Abbreviations: EAD adaxial epidermis, EAB abaxial epidermis, COA angular collenchyma, COL lamellar collenchyma, E endoderm, P phloem, X xylem, FP fundamental parenchyma.

Overall, the anatomical structure of the sample of this study is relatively easily identifiable using the reference image. The cell walls remained intact during the sample preparation, but the morphology appears to have been affected by the dehydration steps, making the cells more erratic compared to those in the reference image. As described earlier, the areas in the samples analyzed with NanoSIMS are marked with green boxes. The three samples that exhibited notable elevated $^{13}C/^{12}C$ ratios were analyzed in the phloem (vascular tissue) of the leaves.

Figure 12a shows the combined ion images of $^{12}C^{14}N$, ^{31}P, and ^{32}S for the sample exposed to UV light and treated with PFOA. The bright spots indicate the presence of nitrogen, phosphorus, and sulfur, while the darker areas indicate absence of these elements, denoting the presence of resin in these areas. The structural distribution is relatively easily identifiable, indicating good preservation of the plant biomass and the cell organelles. Using SEM images and the combined ion images, ROIs were identified. Figure 12b illustrates the ROIs for the sample exposed to UV light and treated with PFOA. The regions of interest were classified into three categories, namely “edges”, “organelles”, and “resin”. Organic structures resembling the walls of the cells were classified as “edges”, internal organic structures within the cell resembling organelles were classified as “organelles”, and areas lacking organic material were assumed to be filled with resin and were therefore classified as “resin”. In this example ROIs 2, 3, 13,

and 15 are classified as edges, ROIs 4, 6, 7, 8, 10, and 16 are classified as organelles, and ROIs 1, 5, 9, 11, 12, 14, 17, and 18 are classified as resin.

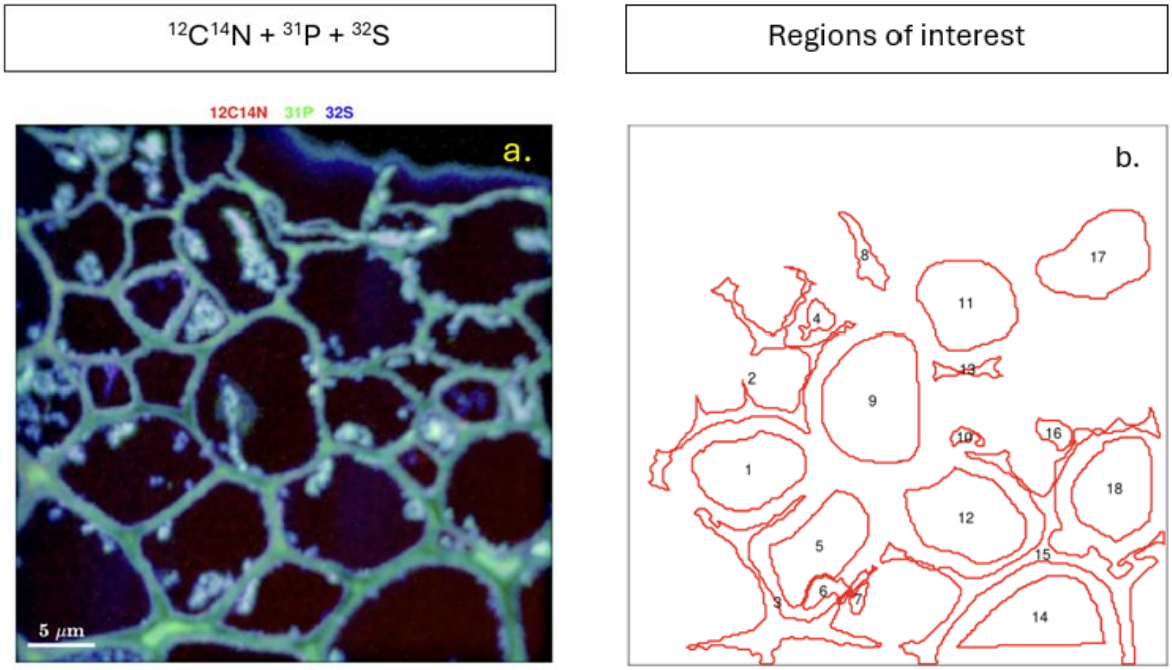

Figure 12: (a) Combined ion $^{12}C^{14}N$, ^{31}P, and ^{32}S for the sample that was exposed to UV light and was treated with PFOA, and (b) the ROIs of this sample.

3.3 Isotope ratio analysis

Figure 13 shows the combined ion images of $^{12}C^{14}N$, ^{31}P, and ^{32}S and the $^{13}C/^{12}C$ ratios of the three analyzed samples. The $^{13}C/^{12}C$ ratios in the sample of the plant that was treated with UV and PFOA (fig. 13a) are notably higher compared to the other two samples. This is likely caused by so-called signal drift, and this drift is corrected during the calculation of the averaged isotopic ratios in the ROIs. The averaged ratios for this sample are 0.01080 and 0.01063 for the edges and organelles, respectively. The sample that was irradiated with UV light and treated with PFOS (fig. 13b) also shows elevated ^{13}C counts in certain regions relative to the natural abundance of ^{13}C of approximately 0.01084. However, the averaged $^{13}C/^{12}C$ ratios of 0.01074 and 0.01069 for the edges and the organelles, respectively are below the natural abundance value. Surprisingly, the sample that was not irradiated with UV light and was not exposed to PFAS (fig. 13c) exhibits relatively high $^{13}C/^{12}C$ ratios of values between 0.0110 and 0.0115 and had similar $^{13}C/^{12}C$ ratios compared to the two samples that were exposed to PFAS, namely 0.01073 for the edges and 0.01062 for the organelles.

$^{12}C^{14}N + {}^{31}P + {}^{32}S$	$^{13}C/^{12}C$ ratio

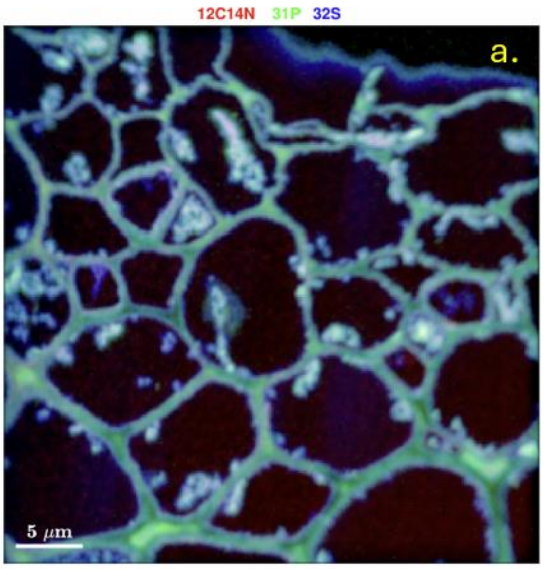

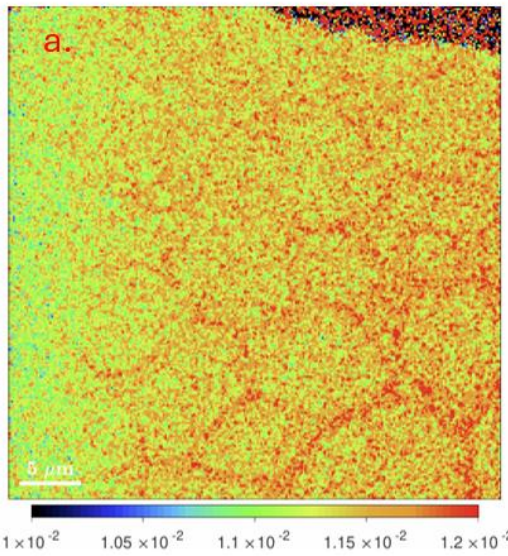

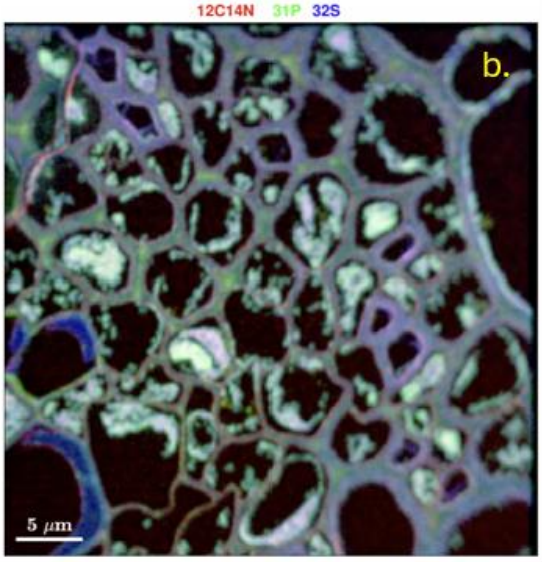

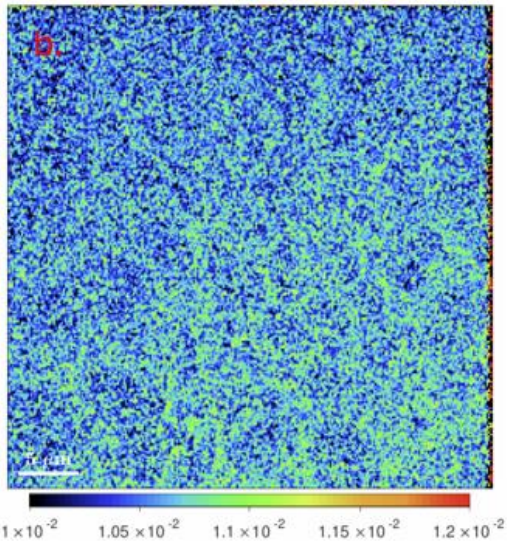

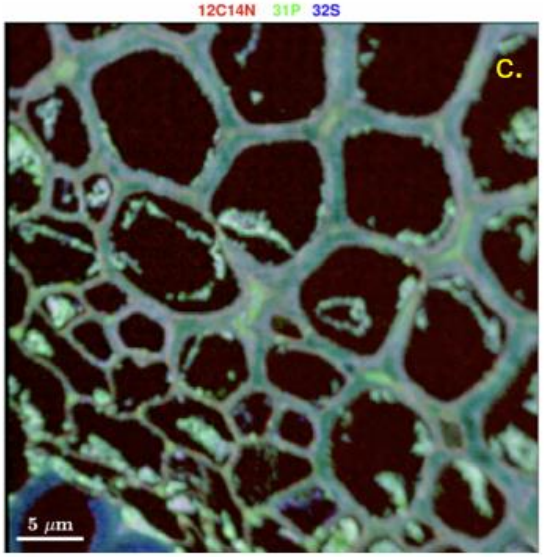

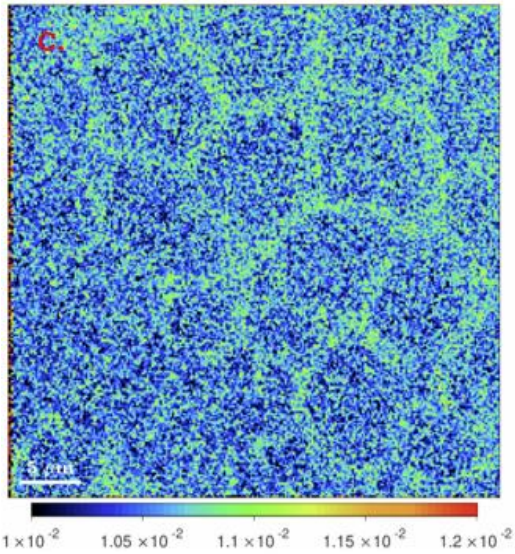

Figure 13: The combined ion images of $^{12}C^{14}N$, ^{31}P, and ^{32}S and the $^{13}C/^{12}C$ ratios of the sample that was (a) treated with UV and PFOA, (b) treated with UV light and treated with PFOS, and (c) not irradiated with UV light and was not exposed to PFAS.

Figure 14 illustrates the $^{19}F/(^{12}C+^{13}C)$ ratios of the three samples. In all samples, significant counts of ^{19}F were detected in the edges. Specifically, in the sample exposed to UV light and PFOA (fig. 14a), various locations exhibited $^{19}F/(^{12}C+^{13}C)$ ratios ranging from 0.12 to 0.15. Additionally, the other two samples also showcased enhanced $^{19}F/(^{12}C+^{13}C)$ ratios in certain locations primarily at the edges, although not as clear as the UV-exposed and PFOA-treated sample.

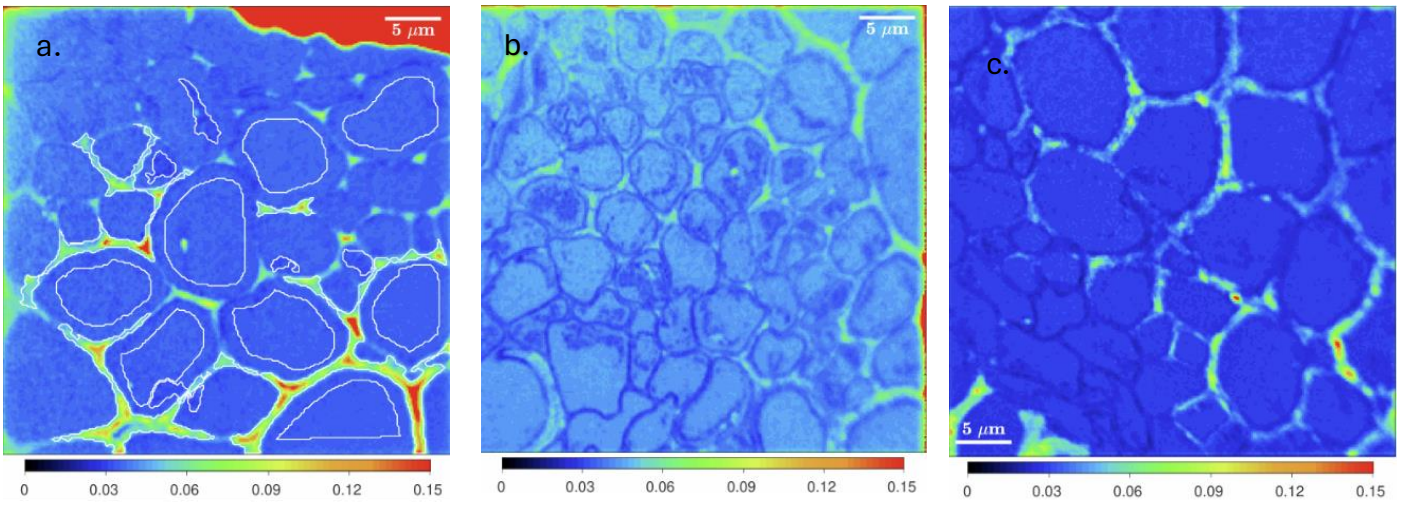

Figure 14: The $^{19}F/(^{12}C+^{13}C)$ ratios of the sample that was (a) treated with UV and PFOA, (b) treated with UV light and treated with PFOS, and (c) not irradiated with UV light and was not exposed to PFAS.

Due to the uncertainty regarding the accumulation of PFAS in the plants, further $^{13}C/F$ ratio analysis to assess potential degradation within the plant tissues (leaves) was abstained from.

Discussion

1. Interpretation of results

1.1 Growth of *Plantago major*

General health of the plants during the study

During the study, the majority of plants appeared healthy and did not seem to be adversely affected by UV light of PFAS exposure. No differences in morphology or coloration of the plants between the two UV treatment groups (+UV and -UV) were observed. The majority of plants in both treatment groups exhibited noticeable growth. New leaves were formed, while older leaves discolored, occasionally leading to full desiccation of the leaf. These findings suggest that the growth of *Plantago major* specimens is likely not influenced by the UV lights they were exposed to in this study. It is worth noting that the UV lights that were used in this study simulate the sun in a desert environment. The ability to survive and even grow in these harsh conditions, contributes to their widespread distribution worldwide even in regions around the equator with very high UV indices (Rojas-Sandoval & Major, 2023). Visually, no morphological changes or discoloration were observed in plants that were exposed to PFOA or PFOS, in comparison to plants that were not exposed to PFAS. These findings indicate that PFOA and PFOS in the concentrations that were used in this study (up to 25 µg/L) do not inhibit or accelerate growth of *Plantago major* and do not exhibit acute toxic effects. This result is in agreement with comparable studies (Gredelj et al., 2020; Zhang et al., 2019; Zhao et al., 2011) Significant phytotoxic effects on *Plantago major* are likely to manifest at much higher PFAS concentrations, typically in the range of mg/L.

Net biomass gain

In this study, no clear correlation was found between the net biomass gain of the plants and the UV treatment (+UV or -UV) they received. In addition, no correlation between the net biomass gain of the plants and the presence of PFAS in their nutrient solution was found. The initial mass of the plants may influence the net biomass gain, as a correlation between the initial mass of the plants and the net biomass gain was found for plants in the +UV treatment. However, this relationship was not observed in the -UV treatment. Biomass is probably not the best indicator for plant growth in this experiment, since the mass of the plants fluctuates due to the formation of new leaves,

growth of existing leaves, and desiccation of old leaves. Desiccation of old leaves seemed to occur faster than growth of new and existing leaves. This also explains why the net biomass gain of a significant amount of plants actually decreased, although plants actually showed visible growth.

Other factors influencing plant growth

It should be noted that the presence of fungi may have influenced the mass and growth of the plants during the study period. The fungi was probably a species of powdery mildew, which is known to cause leaf necrosis (death) (Powdery Mildew - B.M. Cunfer, n.d.) A great amount of plants in both fume hoods were infected by the fungus and leaves that were fully covered with the fungus would quickly desiccate and die. Another variable that may have influenced the growth experiment is seasonality. The study period took place during the winter months in November and December, which is just outside the flowering period of *Plantago major* (Flora van Nederland: Grote Weegbree - Plantago Major s. Major, n.d.). Although the light regime in the fume hoods was simulated, it is important to acknowledge that seasonality may still affect the growth of the plant.

1.2 Bulk Analysis

The significant biological variation in the natural carbon isotopes ratio ($^{13}C/^{12}C$) between plants, made detection of elevated ^{13}C levels in the plant tissues due to incorporated ^{13}C-labelled PFAS impossible. The intended PFAS concentrations in the nutrient solutions (80 mL) of the plants was 25 µg/L, which means that the bioavailability amounted to 2 µg PFAS per plant. Even if a plant absorbed all the bioavailable PFAS, the $\delta^{13}C$ value would only experience minimal increases of approximately 0.06-0.71‰ (text box 2), depending on the total carbon mass of each individual plant. This increase is insufficient to differentiate between natural biological variability between plants and the incorporation of PFAS in the plants, and moreover it is unlikely that PFAS removal efficacies of 100% can be achieved (Awad et al., 2022; Zhang et al., 2019). The PFAS concentration that was used in the study was chosen, since comparable studies used similar concentrations in their exposure experiments. In addition, it is worth noting that ^{13}C-labelled PFOA and PFOS are expensive chemicals. Therefore, increasing their concentrations in the nutrient solutions would have markedly increase costs. Finally, it is important to consider that a higher concentration, for instance, 250 µg/L, could potentially induce toxic effects

on the plants (Gredelj et al., 2020). These effects might influence the growth of the plant and the uptake potential of PFAS. These three factors suggest that EA-IRMS was not a feasible approach for detecting PFAS accumulation in plants.

Theoretical $\delta^{13}C$ increase if plants would have 100% removal efficacy:

The minimum and maximum masses of the plants were approximately 1.5 g and 15 g, respectively. About 90% of this weight is due to water, meaning the dried total weight for the lightest plant would be 0.15 g, and for the heaviest plant, 1.5 g. Since this dried material consists of approximately 40% carbon (C_{nat}), the lightest plant contains about 0.06 g (5000 µmol) of natural carbon, while the heaviest plant contains approximately 0.6 g (50000 µmol) of natural carbon.

This study found that the natural $^{13}C/^{12}C$ ratio (R_{nat}) of Plantago major specimens in this trial is approximately 0.01084 (equation S8).

$$R_{nat} = \frac{13C_{nat}}{12C_{nat}} = 0.01084 \qquad (S8)$$

Where $13C_{nat}$ and $12C_{nat}$ represent the amount of natural ^{13}C and ^{12}C in the plants, respectively, expressed in mmol. The amount of ^{12}C in the plants can be assumed to be equal to C_{nat} - $13C_{nat}$. Substituting this into equation S8 yields equation S9.

$$\frac{13C_{nat}}{C_{nat} - 13C_{nat}} = 0.01084 \qquad (S9)$$

Solving for $13C_{nat}$ yields the following equation:

$$13C_{nat}\ (\mu mol) = \frac{0.01084\ x\ C_{nat}}{1 + 0.01084} \qquad (S10)$$

The 13C mass fractions ($13C_{m,frac}$) in both ^{13}C-labeled PFOA and PFOS were calculated using equation S4.

$$13C_{m,frac,PFAS} = \frac{(n_C * MN_{13C})}{MW_{PFAS}} \qquad (S11)$$

Where n_c is equal to amount of carbon atoms in the respective PFAS molecule (8 for both PFOA and PFOS), MN_{13C} stands for the mass number of ^{13}C (=13), and the MW_{PFAS} denotes the molar weight of the respective PFAS (PFOA = 422, PFOS = 508). If it assumed that 100% of the bioavailable PFAS is removed by the plant, equation S12 can be utilized to calculate the amount of ^{13}C in the PFAS molecules ($13C_{PFAS}$), expressed in µmol.

$$13C_{PFAS}\ (\mu mol) = \frac{13C_{m,frac,PFAS}\ x\ V_{sol}\ x\ PFAS_{conc}}{MN_{13C}} \qquad (S12)$$

With V_{added} equal to the volume of the nutrient solution, expressed as µL (=80000), and $PFAS_{conc}$ representing the PFAS concentration in the nutrient solution (=0.000025), expressed in µg/µL.

The accumulation of the PFAS in the plants raises the $^{13}C/^{12}C$ ratio in the plants. If it assumed that the accumulated PFAS is distributed evenly in the plant tissues, equation S13 can be utilized to calculate the $^{13}C/^{12}C$ ratio in the plants (R_{plant}) after exposure.

$$R_{plant} = \frac{13C_{nat} + 13C_{PFAS}}{12C_{nat}} \qquad (S13)$$

Utilizing equation S13, the following ratios are found for the exposed plants:

Lightest plant: PFOA: 0.0108477, PFOS: 0.0108464
Heaviest plant: PFOS: 0.01084077, PFOS: 0.0108064

Equation S14 provides theoretical $\delta^{13}C$ values for the plant tissues assuming 100% of the bioavailable PFOA/PFOS in the nutrient solution accumulates in the plant. It is important to note that the mass distribution of the PFAS is considered to be even.

Lightest plant: PFOA: +0.71‰, PFOS: +0.61‰
Heaviest plant: PFOA: +0.07‰, PFOS: +0.06‰

$$\delta 13C\ (‰) = \left(\left(\frac{R_{sample}}{R_{nat}}\right) - 1\right) x\ 1000 \qquad (S14)$$

Text box 2: Theoretical $\delta^{13}C$ estimation of plants exposed to PFOA or PFOS during the study period assuming 100% removal efficacy.

1.3 NanoSIMS analysis

Sample preparation

The quality of the NanoSIMS analysis largely depends on the initial preparation of the plant tissues, making the sample preparation a crucial step in the process. Out of the eighteen samples of *Plantago major* plant tissues prepared to be analyzed with NanoSIMS, only six were suitable for analysis. The SEM images (fig. 10) of the samples revealed the presence of visible damage to the cell structure of the tissues. However, well-preserved areas of the plant tissues were still detectable and suitable for analysis. A great concern of the preservation of the plant tissues was the fact that plants were frozen (-20°C). Freezing the tissues may have caused the formation of ice crystals in the cells and organelles of the plants, which can lead to redistribution of analytes (Dong et al., 2016). During the optimization of the sample preparation, frozen tissues were compared to fresh tissues (Fig. 15). The sample containing fresh plant tissues (Fig. 15a) exhibited visibly better-preserved cell structures compared to the sample that had

been frozen prior to sample preparation (Fig. 15b). It is likely that ice crystal formation occurred in the frozen sample, leading to damage to the tissue structure.

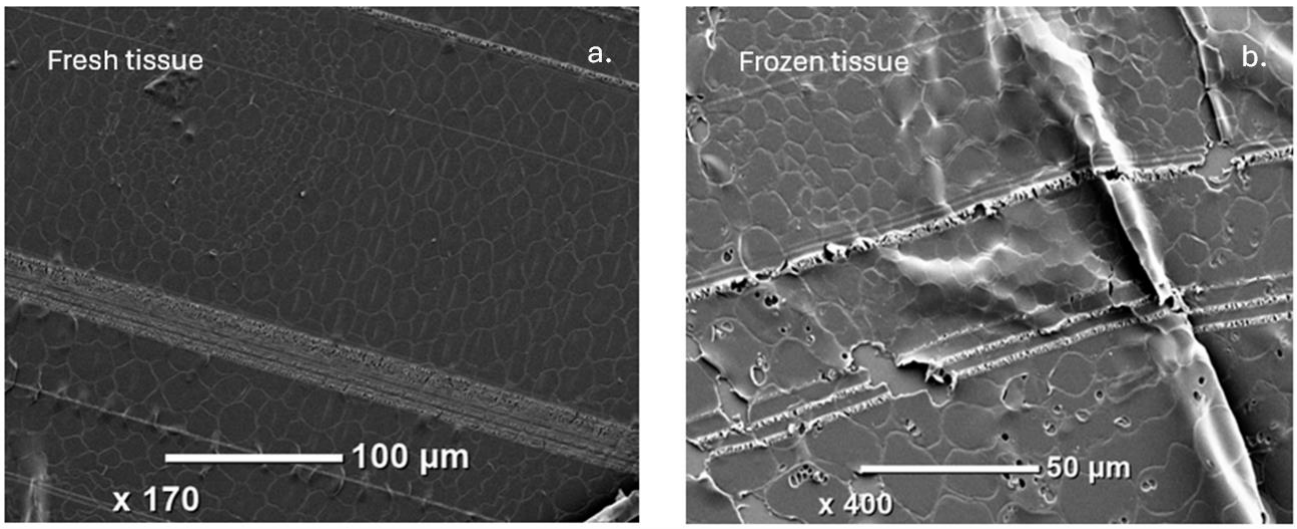

Figure 15: SEM images of a (a) plant tissue that was freshly chemically fixated, and a (b) plant tissue that was frozen before chemical fixation.

The samples from the exposure experiments (UV and PFAS) were harvested, before the sample preparation methodology was fully optimized. To prevent decay of the plants, they were stored in the freezer before further sample preparation. Therefore it is likely that the plants from the exposure experiments sustained some level of physical damage to the cell structures, which potentially led to redistribution of accumulated PFAS. This redistribution influences the spatial distribution of accumulated PFAS and might even result in the loss of accumulated PFAS due to washings after freezing.

$^{13}C/^{12}C$ ratios

Only samples that contained leaves of the plant were included in the analysis. This decision was based on the hypothesis that potential PFAS degradation would occur in the leaves of the plant, since these tissues were directly irradiated with UV light. Among these samples, three exhibited notable elevated $^{13}C/^{12}C$ ratio counts at certain locations within the leaf. These samples include a plant that was exposed to UV light and PFOA, a plant that was exposed to UV light and PFOS, and a plant that underwent neither UV exposure nor exposure to PFAS. In the other samples no notable elevated $^{13}C/^{12}C$ ratios were visible, which is surprising since these samples were also exposed to PFAS.

The results of the bulk analysis showed that the average $\delta^{13}C$ for the plant leaves that received no UV treatment and were not exposed to PFAS was approximately -30.89 ‰. This corresponds to a $^{13}C/^{12}C$ ratio of approximately 0.01084, which can be regarded as the natural ratio for leaves of *Plantago major*. As described in the results from the NanoSIMS analysis, the ROIs were divided into edges, organelles and resin. The edges represent the cell walls of the plants, while the organelles represent the various intracellular structures, such as the nucleus, mitochondria, and chloroplasts. Additionally, the resin areas indicate regions filled with resin during the sample preparation. The averaged $^{13}C/^{12}C$ ratios of the organic plant material (cell walls and organelles) did not exceed the average $^{13}C/^{12}C$ ratio of 0.01084 (estimated with bulk analysis) in any of the three samples. That being said, the $^{13}C/^{12}C$ isotope images (fig. 13) reveal locations, primarily within the cell walls, where elevated $^{13}C/^{12}C$ ratios counts up to 0.0120 are observed, particularly in the sample that received UV treatment and was exposed to PFOA (fig. 13a). The other two samples (fig. 13b & fig. 13c) exhibit less clear enhanced $^{13}C/^{12}C$ ratios compared to the first sample. However, ratios of up to 0.0110 and possibly even higher can be still be observed. Based on these findings, it is challenging to implicate whether PFAS truly had accumulated in the plants that showed enhanced $^{13}C/^{12}C$ ratios.

A $^{13}C/^{12}C$ ratio of 0.0120 ($\delta^{13}C$ ~ 70) does not occur naturally in plants, so this enrichment indicates that PFOA was taken up in this plant and accumulated mainly in the cell walls of the plant. That being said, the $^{13}C/^{12}C$ ratios of the ROIs in this image appear to be generally higher in comparison to the other two samples. Even the ROIs that are classified as resin display elevated ratios. Given that this pattern is consistent throughout the entire image and not observed in the other two images, it is possible that the image may have been processed incorrectly. This is called drift, and this drift is corrected for when calculating the average ratios for the ROIs. Alternatively, although unlikely, it is possible that the resin of this sample was contaminated with PFOA during the sample preparation, which could explain the enhanced $^{13}C/^{12}C$ ratios of the resin in this sample, relative to the other two samples. The sample that was exposed with UV light and PFOS (fig 13b), exhibits notable enhanced $^{13}C/^{12}C$ ratios (although not as clear as the other two samples). Assuming that the increased ratios are a result of PFOS enrichment, a possible explanation for the fact that this sample shows less prominent $^{13}C/^{12}C$ ratios, compared to the sample that was exposed to PFOA

(fig. 13a) could be that PFOS tends accumulate in the roots of plants. This is unlike PFOA, which tends to accumulate more in the shoots of plants (Wang et al., 2020).

The elevated $^{13}C/^{12}C$ ratios in the untreated sample (fig. 13c) indicate that the increased ratios found in the other two samples may not be attributed to PFAS accumulation. Instead, these elevated $^{13}C/^{12}C$ ratios might be naturally occurring in certain plants or specific regions of plants. However, it is unlikely that plants naturally exhibit such considerable fluctuations in $^{13}C/^{12}C$ ratios. Therefore, it is possible that errors, such as mixing up the samples during preparation, might have occurred.

Presence of Fluorine

Since assessing whether PFAS accumulation actually occurred in the plants by just using the $^{13}C/^{12}C$ ratio is challenging, the $^{19}F/(^{12}C+^{13}C)$ ratio was used as an additional proxy for PFAS accumulation. In fig. 14a, the sample subjected to UV and PFOA treatments exhibits multiple regions where the $^{19}F/(^{12}C+^{13}C)$ ratio counts are 0.15 or possibly even higher. Similarly, the sample without UV and/or PFAS treatment (fig. 14c), also displays such regions, although to a lesser extent. Assuming that the plant tissues consist of approximately 40% carbon, this corresponds to a fluorine fraction of 6%. This observed fraction greatly exceeds the natural fluorine content in vegetables, as determined by a 2021 study, which averages around 0.01 mg/kg or 0.01 ppm (Jarosz & Pitura, 2021). Therefore the elevated fluorine levels in the samples suggest accumulation of PFAS. That being said, it is important to state that the results from NanoSIMS analysis are semi-quantitative. The values displayed in the ratio images are not true elemental ratios. It serves as an indicator for elevated concentrations of isotopes in certain regions, but the values are not accurate.

During the optimization of the sample preparation for the NanoSIMS, elevated $^{19}F/(^{12}C+^{13}C)$ ratios were found in various samples (fig. 16). These samples were never exposed to PFAS, which questions whether the unusually high ratios are attributed to PFAS accumulation or if another explanation is more plausible. Figure 16 illustrates the $^{19}F/(^{12}C+^{13}C)$ ratios of a root (fig. 16) and a leaf (fig. 16b), which were utilized to assess the quality of the plant tissues sample preparation method for the NanoSIMS. Both samples exhibit abnormally high $^{19}F/(^{12}C+^{13}C)$ ratios similar to the previously mentioned samples. Based on these results, the elevated $^{19}F/(^{12}C+^{13}C)$ ratios in the samples that were exposed to PFAS cannot be directly attributed to accumulated PFAS in the plant tissues.

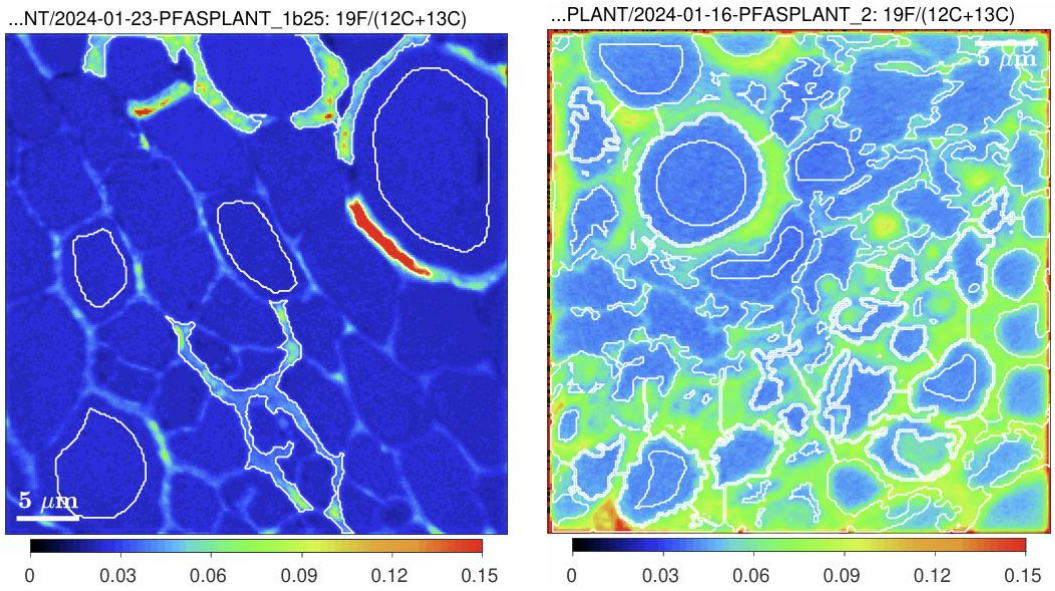

Figure 15: The $^{19}F/(^{12}C+^{13}C)$ ratios of two samples that were not exposed to PFAS.

2. Limitations of the Study and future directions

2.1 Experimental design plant growth

Hydroponics versus solid matrix

For this study, a hydroponic growing system was utilized to cultivate plant specimens of *Plantago major*. Only the roots of the plants were in direct contact with the nutrient solution. For the exposure experiments, PFOA or PFOS was added to the nutrient solutions. The benefits of hydroponics include a more controlled environment and higher bioavailability of PFAS compared to solid matrices where adsorption plays a significant role. Hydroponics are employed in this study, since it was solely based on the bioaccumulation potential of PFAS in *Plantago major*. However, when assessing the phytoremediation potential of *Plantago major* in PFAS-contaminated sites, soil-based growth experiments should be conducted to simulate realistic situations. In soils, sorption becomes a prominent process that affects the availability of PFAS to plant roots, thereby influencing the PFAS accumulation potential in *Plantago major*.

Proxy for plant growth

To determine the influence of UV light and PFAS on the growth of the plant, the net biomass gain (plant mass at harvest – initial plant mass) was determined and utilized as a proxy for the growth of plant. However, this approach proved to be unreliable, since the mass of the plants fluctuates due to the formation of new leaves, growth of existing leaves, and desiccation of old leaves. In future research, a visual representation of the plant growth, such as before and after photos or a time-lapse video may be a better proxy.

2.2 EA-IRMS analysis

In this study, elemental analyzer isotope ratio mass spectrometry (EA-IRMS) was utilized to quantify the bulk concentration of accumulated PFAS in the different plant tissues of *Plantago major*. Plants were exposed to ^{13}C-labelled PFAS, with the anticipation that the $^{13}C/^{12}C$ ratio of the plant tissues would increase significantly due to accumulation of PFAS. However, the biological variance of the $^{13}C/^{12}C$ ratio among different plants exceeded the expected increases attributed to the presence of PFAS, resulting in statistically insignificant results. This finding is supported by a 2017 study, which also observed significant biological variance in $\delta^{13}C$ (Cennerazzo et al., 2017).

Assuming that all PFAS present in the nutrient solutions would be taken up by the plants, a tenfold increase in the initial PFAS concentration in the nutrient would likely be required to cause any significant increases in the $^{13}C/^{12}C$ ratio of exposed plants. Using EA-IRMS to estimate the bulk concentration of accumulated PFAS in plants is probably not a feasible method. Comparable studies typically employed extraction methods to extract the accumulated PFAS from dried samples. Subsequently, the supernatants obtained from the extractions were analyzed using a combination of high performance liquid chromatography (HPLC) and mass spectrometry (MS) to quantify the PFAS concentrations (Awad et al., 2022; Felizeter et al., 2012; Gredelj et al., 2020). Although EA-IRMS is a potential cost-effective method to quantify accumulated PFAS concentrations, extraction followed by HPLC-MS is a more effective approach to detect lower, more realistic PFAS concentrations. Future studies should therefore employ extraction methods combined with HPLC-MS.

2.3 NanoSIMS sample preparation

After harvesting the plants, they were stored in a freezer at -20°C for an extended period to prevent decay. However, freezing the samples may have damaged the cells of the plants, which potentially caused redistribution of metabolites and accumulated PFAS. This redistribution could alter the spatial distribution of accumulated PFAS within the plants and may even result in losses or washing away of PFAS from the plant tissues. Future research should preferably involve sectioning the plants immediately after harvesting. The sections should then be thoroughly washed, followed by immediate chemical fixation. After chemical fixation, the samples can be stored at -80°C before further sample preparation. Rapid chemical fixation of the plant tissues after harvesting serves to minimize redistribution of PFAS within the tissues and also preserves the cell structure more effectively.

2.4 Potential PFAS degradation

The current study initially anticipated to compare the NanoSIMS data of $^{13}C/^{12}C$ ratios with the $^{13}C/F$ ratios of the plants. Since PFAS the will be fully ^{13}C-labeled, it has a specific $^{13}C/F$ ratio. If PFAS becomes degraded, fully or partially, one or more of the F atoms will separate from the ^{13}C atom. If the F atom is transported through the plant while the ^{13}C atom is “left behind”, the $^{13}C/F$ ratio will increase in the areas where PFAS is localized within the plant tissue. However, due to the uncertainty regarding the accumulation of PFAS in the plants, further interpretations concerning the potential

degradation of PFAS within the plant tissues were abstained from. In addition, according to the literature, the potential of degradation in plants is probably very low (Kavusi et al., 2023). Even if degradation were to occur it is anticipated that the amount of degraded PFAS is minimal, possibly a few percent. This level of degradation is unlikely to be detectable using NanoSIMS. A better approach would be to use HPLC-MS to detect any degradation residual products of PFOA and PFOS, which may include shorter chain PFAS such as PFBA or TFA, or perfluorocarbons such as tetrafluoromethane (CF_4). Another possibility is to analyze the CO_2 that is emitted by the plants. Elevated $^{13}C/^{12}C$ ratios in the emitted CO_2 indicate possible mineralization of PFAS.

Conclusion

This study aimed to investigate whether perfluorooctanoic acid (PFOA) and perfluorooctanesulfonic acid (PFOS) can accumulate and subsequently be degraded in plant tissues (leaves, stems, and roots) irradiated with UV light. In addition, this study aimed to evaluate the impact of UV and/or PFAS exposure on the health of *Plantago major* specimens. Neither the presence of UV light nor PFOA or PFOS seemed to affect the health of *Plantago major* specimens. Throughout the study period, there were no observable morphological changes, discoloration, or inhibited growth in the plants. The net biomass gain (plant mass at harvest – initial plant mass) was estimated of every plant, but proved to be ineffective as a proxy for plant growth. No PFAS accumulation was detected via EA-IRMS analysis, since the biological variance of the $^{13}C/^{12}C$ ratio among different plants exceeded the expected increases attributed to the presence of PFAS. Although EA-IRMS offers potential as a quick and cost-effective method for detecting ^{13}C-labelled PFAS in organic tissues, the low bioaccumulation concentration did not result in significant changes in the $^{13}C/^{12}C$ ratios of the plants. Analysis of both $^{13}C/^{12}C$ ratios and $^{19}F/(^{12}C+^{13}C)$ ratios in plant tissues, which were obtained through NanoSIMS analysis, revealed possible accumulation of both PFOA and PFOS in the leaves of several plants. However, elevated ratios were also detected in a leaf of a plant that did not receive UV or PFAS treatments. In addition, several samples exposed to PFAS did not exhibit elevated ratios. Hence, the elevated ratios in some of the samples cannot solely be attributed to PFAS accumulation in plant tissues. Given the uncertainty surrounding the accumulation of PFAS in the plants, further interpretations concerning the potential degradation of PFAS within the plant tissues (leaves) were abstained from.

References

Abunada, Z., Alazaiza, M. Y. D., & Bashir, M. J. K. (2020). An Overview of Per- and Polyfluoroalkyl Substances (PFAS) in the Environment: Source, Fate, Risk and Regulations. Water 2020, Vol. 12, Page 3590, 12(12), 3590. https://doi.org/10.3390/W12123590

Adu, O., Ma, X., & Sharma, V. K. (2023). Bioavailability, phytotoxicity and plant uptake of per- and polyfluoroalkyl substances (PFAS): A review. *Journal of Hazardous Materials*, *447*, 130805. https://doi.org/10.1016/j.jhazmat.2023.130805

Ahrens, L., & Bundschuh, M. (2014). Fate and effects of poly- and perfluoroalkyl substances in the aquatic environment: A review. *Environmental Toxicology and Chemistry*, *33*(9), 1921–1929. https://doi.org/10.1002/etc.2663

Ahrens, L., Taniyasu, S., Yeung, L. W. Y., Yamashita, N., Lam, P. K. S., & Ebinghaus, R. (2010). Distribution of polyfluoroalkyl compounds in water, suspended particulate matter and sediment from Tokyo Bay, Japan. *Chemosphere*, *79*(3), 266–272. https://doi.org/10.1016/J.CHEMOSPHERE.2010.01.045

Ali, H., Khan, E., & Sajad, M. A. (2013). Phytoremediation of heavy metals-Concepts and applications. In *Chemosphere* (Vol. 91, Issue 7, pp. 869–881). Elsevier Ltd. https://doi.org/10.1016/j.chemosphere.2013.01.075

Allred, B. M. K., Lang, J. R., Barlaz, M. A., & Field, J. A. (2015). Physical and Biological Release of Poly- and Perfluoroalkyl Substances (PFASs) from Municipal Solid Waste in Anaerobic Model Landfill Reactors. *Environmental Science and Technology*, *49*(13), 7648–7656. https://doi.org/10.1021/ACS.EST.5B01040

Awad, J., Brunetti, G., Juhasz, A., Williams, M., Navarro, D., Drigo, B., Bougoure, J., Vanderzalm, J., & Beecham, S. (2022). Application of native plants in constructed floating wetlands as a passive remediation approach for PFAS-impacted surface water. *Journal of Hazardous Materials*, *429*, 128326. https://doi.org/10.1016/j.jhazmat.2022.128326

Banayan Esfahani, E., Asadi Zeidabadi, F., Zhang, S., & Mohseni, M. (2022a). Photo-chemical/catalytic oxidative/reductive decomposition of per- and poly-fluoroalkyl substances (PFAS), decomposition mechanisms and effects of key factors: a review. *Environmental Science: Water Research & Technology*, *8*(4), 698–728. https://doi.org/10.1039/D1EW00774B

Banayan Esfahani, E., Asadi Zeidabadi, F., Zhang, S., & Mohseni, M. (2022b). Photo-chemical/catalytic oxidative/reductive decomposition of per- and poly-fluoroalkyl substances (PFAS), decomposition mechanisms and effects of key factors: a review.

Environmental Science: Water Research & Technology, *8*(4), 698–728. https://doi.org/10.1039/D1EW00774B

Bolan, N., Sarkar, B., Yan, Y., Li, Q., Wijesekara, H., Kannan, K., Tsang, D. C. W., Schauerte, M., Bosch, J., Noll, H., Ok, Y. S., Scheckel, K., Kumpiene, J., Gobindlal, K., Kah, M., Sperry, J., Kirkham, M. B., Wang, H., Tsang, Y. F., … Rinklebe, J. (2021). Remediation of poly- and perfluoroalkyl substances (PFAS) contaminated soils – To mobilize or to immobilize or to degrade? *Journal of Hazardous Materials*, *401*. https://doi.org/10.1016/j.jhazmat.2020.123892

Brendel, S., Fetter, É., Staude, C., Vierke, L., & Biegel-Engler, A. (2018). Short-chain perfluoroalkyl acids: environmental concerns and a regulatory strategy under REACH. *Environmental Sciences Europe*, *30*(1), 1–11. https://doi.org/10.1186/S12302-018-0134-4/FIGURES/2

Brusseau, M. L., Anderson, R. H., & Guo, B. (2020). *PFAS concentrations in soils: Background levels versus contaminated sites*. https://doi.org/10.1016/j.scitotenv.2020.140017

Buck, R. C., Franklin, J., Berger, U., Conder, J. M., Cousins, I. T., Voogt, P. De, Jensen, A. A., Kannan, K., Mabury, S. A., & van Leeuwen, S. P. J. (2011). Perfluoroalkyl and polyfluoroalkyl substances in the environment: Terminology, classification, and origins. *Integrated Environmental Assessment and Management*, *7*(4), 513–541. https://doi.org/10.1002/IEAM.258

Cennerazzo, J., de Junet, A., Audinot, J. N., & Leyval, C. (2017). Dynamics of PAHs and derived organic compounds in a soil-plant mesocosm spiked with 13C-phenanthrene. Chemosphere, 168, 1619–1627. https://doi.org/10.1016/J.CHEMOSPHERE.2016.11.145

Costello, M. C. S., & Lee, L. S. (2020). Sources, Fate, and Plant Uptake in Agricultural Systems of Per- and Polyfluoroalkyl Substances. In *Current Pollution Reports*. Springer Science and Business Media Deutschland GmbH. https://doi.org/10.1007/s40726-020-00168-y

Dasu, K., Xia, X., Siriwardena, D., Klupinski, T. P., & Seay, B. (2022). Concentration profiles of per- and polyfluoroalkyl substances in major sources to the environment. *Journal of Environmental Management*, *301*, 113879. https://doi.org/10.1016/J.JENVMAN.2021.113879

De Silva, A. O., Armitage, J. M., Bruton, T. A., Dassuncao, C., Heiger-Bernays, W., Hu, X. C., Kärrman, A., Kelly, B., Ng, C., Robuck, A., Sun, M., Webster, T. F., & Sunderland, E. M. (2021). PFAS Exposure Pathways for Humans and Wildlife: A Synthesis of Current Knowledge and Key Gaps in Understanding. In *Environmental Toxicology and Chemistry* (Vol. 40, Issue 3, pp. 631–657). Wiley Blackwell. https://doi.org/10.1002/etc.4935

Dhore, R., & Murthy, G. S. (2021). Per/polyfluoroalkyl substances production, applications and environmental impacts. *Bioresource Technology*, *341*, 125808. https://doi.org/10.1016/j.biortech.2021.125808

Dong, Y., Li, B., Malitsky, S., Rogachev, I., Aharoni, A., Kaftan, F., Svatoš, A., & Franceschi, P. (2016). Sample preparation for mass spectrometry imaging of plant tissues: A review. *Frontiers in Plant Science*, *7*(FEB2016), 170331. https://doi.org/10.3389/FPLS.2016.00060/BIBTEX

Etim, E., & Etim, E. E. (2012). Phytoremediation and Its Mechanisms: A Review. *International Journal of Environment and Bioenergy*, *2012*(3), 120–136. https://www.researchgate.net/publication/312443920

Evich, M. G., Davis, M. J. B., McCord, J. P., Acrey, B., Awkerman, J. A., Knappe, D. R. U., Lindstrom, A. B., Speth, T. F., Tebes-Stevens, C., Strynar, M. J., Wang, Z., Weber, E. J., Henderson, W. M., & Washington, J. W. (2022). Per- and polyfluoroalkyl substances in the environment. *Science*, *375*(6580). https://doi.org/10.1126/science.abg9065

Faust, J. A. (2023). *PFAS on atmospheric aerosol particles: a review*. https://doi.org/10.1039/d2em00002d

Felizeter, S., McLachlan, M. S., & De Voogt, P. (2012). Uptake of perfluorinated alkyl acids by hydroponically grown lettuce (Lactuca sativa). *Environmental Science and Technology*, *46*(21), 11735–11743. https://doi.org/10.1021/ES302398U/SUPPL_FILE/ES302398U_SI_001.PDF

Flora van Nederland: Grote weegbree - Plantago major s. major. (n.d.). Retrieved April 1, 2024, from https://www.floravannederland.nl/planten/grote_weegbree

Gaballah, S., Swank, A., Sobus, J. R., Howey, X. M., Schmid, J., Catron, T., McCord, J., Hines, E., Strynar, M., & Tal, T. (2020). Evaluation of developmental toxicity, developmental neurotoxicity, and tissue dose in zebrafish exposed to genX and other PFAS. *Environmental Health Perspectives*, *128*(4). https://doi.org/10.1289/EHP5843/SUPPL_FILE/EHP5843.S002.CODEANDDATA.ACCO.ZIP

Gagliano, E., Sgroi, M., Falciglia, P. P., Vagliasindi, F. G. A., & Roccaro, P. (2020). Removal of poly- and perfluoroalkyl substances (PFAS) from water by adsorption: Role of PFAS chain length, effect of organic matter and challenges in adsorbent regeneration. *Water Research*, *171*, 115381. https://doi.org/10.1016/J.WATRES.2019.115381

Gaines, L. G. T. (2023). Historical and current usage of per- and polyfluoroalkyl substances (PFAS): A literature review. In *American Journal of Industrial Medicine* (Vol. 66, Issue 5, pp. 353–378). John Wiley and Sons Inc. https://doi.org/10.1002/ajim.23362

Ghisi, R., Vamerali, T., & Manzetti, S. (2018). *Accumulation of perfluorinated alkyl substances (PFAS) in agricultural plants: A review*. https://doi.org/10.1016/j.envres.2018.10.023

Glüge, J., Scheringer, M., Cousins, I. T., Dewitt, J. C., Goldenman, G., Herzke, D., Lohmann, R., Ng, C. A., Trier, X., & Wang, Z. (2020). An overview of the uses of per- and polyfluoroalkyl

substances (PFAS). *Environmental Science: Processes & Impacts*, *22*(12), 2345–2373. https://doi.org/10.1039/D0EM00291G

Gobelius, L., Lewis, J., & Ahrens, L. (2017). Plant Uptake of Per- and Polyfluoroalkyl Substances at a Contaminated Fire Training Facility to Evaluate the Phytoremediation Potential of Various Plant Species. *Environmental Science and Technology*, *51*(21), 12602–12610. https://doi.org/10.1021/ACS.EST.7B02926/SUPPL_FILE/ES7B02926_SI_001.PDF

Gredelj, A., Nicoletto, C., Polesello, S., Ferrario, C., Valsecchi, S., Lava, R., Barausse, A., Zanon, F., Palmeri, L., Guidolin, L., & Bonato, M. (2020). Uptake and translocation of perfluoroalkyl acids (PFAAs) in hydroponically grown red chicory (Cichorium intybus L.): Growth and developmental toxicity, comparison with growth in soil and bioavailability implications. *Science of The Total Environment*, *720*, 137333. https://doi.org/10.1016/j.scitotenv.2020.137333

Greger, M., & Landberg, T. (2024). Removal of PFAS from water by aquatic plants. *Journal of Environmental Management*, *351*, 119895. https://doi.org/10.1016/j.jenvman.2023.119895

Guo, J., Zhou, J., Liu, S., Shen, L., Liang, X., Wang, T., & Zhu, L. (2022). Underlying Mechanisms for Low-Molecular-Weight Dissolved Organic Matter to Promote Translocation and Transformation of Chlorinated Polyfluoroalkyl Ether Sulfonate in Wheat. *Environmental Science and Technology*, *56*(22), 15617–15626. https://doi.org/10.1021/ACS.EST.2C04356/ASSET/IMAGES/LARGE/ES2C04356_0005.JPEG

Hamid, H., Li, L. Y., & Grace, J. R. (2018). Review of the fate and transformation of per- and polyfluoroalkyl substances (PFASs) in landfills. *Environmental Pollution*, *235*, 74–84. https://doi.org/10.1016/J.ENVPOL.2017.12.030

Haukås, M., Berger, U., Hop, H., Gulliksen, B., & Gabrielsen, G. W. (2007). Bioaccumulation of per- and polyfluorinated alkyl substances (PFAS) in selected species from the Barents Sea food web. *Environmental Pollution*, *148*(1), 360–371. https://doi.org/10.1016/J.ENVPOL.2006.09.021

He, Q., Yan, Z., Qian, S., Xiong, T., Grieger, K. D., Wang, X., Liu, C., & Zhi, Y. (2023). Phytoextraction of per- and polyfluoroalkyl substances (PFAS) by weeds: Effect of PFAS physicochemical properties and plant physiological traits. *Journal of Hazardous Materials*, *454*, 131492. https://doi.org/10.1016/j.jhazmat.2023.131492

Høisæter, Å., Pfaff, A., & Breedveld, G. D. (2019). Leaching and transport of PFAS from aqueous film-forming foam (AFFF) in the unsaturated soil at a firefighting training facility under cold climatic conditions. *Journal of Contaminant Hydrology*, *222*, 112–122. https://doi.org/10.1016/J.JCONHYD.2019.02.010

Jarosz, Z., & Pitura, K. (2021). Fluoride toxicity limit—can the element exert a positive effect on plants? *Sustainability (Switzerland)*, *13*(21). https://doi.org/10.3390/SU132112065

Kafle, A., Timilsina, A., Gautam, A., Adhikari, K., Bhattarai, A., & Aryal, N. (2022). *Phytoremediation: Mechanisms, plant selection and enhancement by natural and synthetic agents*. https://doi.org/10.1016/j.envadv.2022.100203

Kavusi, E., Shahi Khalaf Ansar, B., Ebrahimi, S., Sharma, R., Ghoreishi, S. S., Nobaharan, K., Abdoli, S., Dehghanian, Z., Asgari Lajayer, B., Senapathi, V., Price, G. W., & Astatkie, T. (2023). Critical review on phytoremediation of polyfluoroalkyl substances from environmental matrices: Need for global concern. *Environmental Research*, *217*, 114844. https://doi.org/10.1016/J.ENVRES.2022.114844

Khan, S., Masoodi, T. H., Pala, N. A., Murtaza, S., Mugloo, J. A., Sofi, P. A., Zaman, M. U., Kumar, R., & Kumar, A. (2023). Phytoremediation Prospects for Restoration of Contamination in the Natural Ecosystems. In *Water (Switzerland)* (Vol. 15, Issue 8). MDPI. https://doi.org/10.3390/w15081498

Kucharzyk, K. H., Darlington, R., Benotti, M., Deeb, R., & Hawley, E. (2017). Novel treatment technologies for PFAS compounds: A critical review. *Journal of Environmental Management*, *204*, 757–764. https://doi.org/10.1016/j.jenvman.2017.08.016

Lee, Y. M., Lee, J. Y., Kim, M. K., Yang, H., Lee, J. E., Son, Y., Kho, Y., Choi, K., & Zoh, K. D. (2020). Concentration and distribution of per- and polyfluoroalkyl substances (PFAS) in the Asan Lake area of South Korea. *Journal of Hazardous Materials*, *381*, 120909. https://doi.org/10.1016/J.JHAZMAT.2019.120909

Lenka, S. P., Kah, M., & Padhye, L. P. (2021). A review of the occurrence, transformation, and removal of poly- and perfluoroalkyl substances (PFAS) in wastewater treatment plants. *Water Research*, *199*, 117187. https://doi.org/10.1016/J.WATRES.2021.117187

Lewis, A. J., Yun, X., Spooner, D. E., Kurz, M. J., McKenzie, E. R., & Sales, C. M. (2022). Exposure pathways and bioaccumulation of per- and polyfluoroalkyl substances in freshwater aquatic ecosystems: Key considerations. *Science of The Total Environment*, *822*, 153561. https://doi.org/10.1016/J.SCITOTENV.2022.153561

Mahinroosta, R., & Senevirathna, L. (2020). A review of the emerging treatment technologies for PFAS contaminated soils. In *Journal of Environmental Management* (Vol. 255). Academic Press. https://doi.org/10.1016/j.jenvman.2019.109896

Martin, J. W., Mabury, S. A., Solomon, K. R., & Muir, D. C. G. (2003). Bioconcentration and tissue distribution of perfluorinated acids in rainbow trout (Oncorhynchus mykiss). *Environmental Toxicology and Chemistry*, *22*(1), 196–204. https://doi.org/10.1002/ETC.5620220126

Mayakaduwage, S., Ekanayake, A., Kurwadkar, S., Rajapaksha, A. U., & Vithanage, M. (2022). Phytoremediation prospects of per- and polyfluoroalkyl substances: A review. *Environmental Research*, *212*. https://doi.org/10.1016/j.envres.2022.113311

Meegoda, J. N., Kewalramani, J. A., Li, B., & Marsh, R. W. (2020). A Review of the Applications, Environmental Release, and Remediation Technologies of Per- and Polyfluoroalkyl Substances. *International Journal of Environmental Research and Public Health 2020, Vol. 17, Page 8117*, *17*(21), 8117. https://doi.org/10.3390/IJERPH17218117

Mendez, M. O., & Maier, R. M. (2008). Phytostabilization of mine tailings in arid and semiarid environments - An emerging remediation technology. *Environmental Health Perspectives*, *116*(3), 278–283. https://doi.org/10.1289/ehp.10608

Milley, S. A., Koch, I., Fortin, P., Archer, J., Reynolds, D., & Weber, K. P. (2018). Estimating the number of airports potentially contaminated with perfluoroalkyl and polyfluoroalkyl substances from aqueous film forming foam: A Canadian example. *Journal of Environmental Management*, *222*, 122–131. https://doi.org/10.1016/J.JENVMAN.2018.05.028

Möller, A., Ahrens, L., Surm, R., Westerveld, J., Van Der Wielen, F., Ebinghaus, R., & De Voogt, P. (2010). Distribution and sources of polyfluoroalkyl substances (PFAS) in the River Rhine watershed. *Environmental Pollution*, *158*(10), 3243–3250. https://doi.org/10.1016/J.ENVPOL.2010.07.019

Nakayama, S. F., Yoshikane, M., Onoda, Y., Nishihama, Y., Iwai-Shimada, M., Takagi, M., Kobayashi, Y., & Isobe, T. (2019). Worldwide trends in tracing poly- and perfluoroalkyl substances (PFAS) in the environment. *TrAC Trends in Analytical Chemistry*, *121*, 115410. https://doi.org/10.1016/J.TRAC.2019.02.011

Navarro, I., de la Torre, A., Sanz, P., Pro, J., Carbonell, G., & Martínez, M. de los Á. (2016). Bioaccumulation of emerging organic compounds (perfluoroalkyl substances and halogenated flame retardants) by earthworm in biosolid amended soils. *Environmental Research*, *149*, 32–39. https://doi.org/10.1016/J.ENVRES.2016.05.004

Nazmul Ehsan, M., Riza, M., Pervez, N., Li, C.-W., Zorpas, A. A., & Naddeo, V. (2024). *PFAS contamination in soil and sediment: Contribution of sources and environmental impacts on soil biota*. https://doi.org/10.1016/j.cscee.2024.100643

Panieri, E., Baralic, K., Djukic-Cosic, D., Djordjevic, A. B., & Saso, L. (2022). PFAS Molecules: A Major Concern for the Human Health and the Environment. *Toxics 2022, Vol. 10, Page 44*, *10*(2), 44. https://doi.org/10.3390/TOXICS10020044

Pilon-Smits, E. (2005). PHYTOREMEDIATION. *Https://Doi-Org.Proxy.Library.Uu.Nl/10.1146/Annurev.Arplant.56.032604.144214*, *56*, 15–39. https://doi.org/10.1146/ANNUREV.ARPLANT.56.032604.144214

Polerecky, L., Adam, B., Milucka, J., Musat, N., Vagner, T., & Kuypers, M. M. M. (2012). Look@NanoSIMS – a tool for the analysis of nanoSIMS data in environmental microbiology. *Environmental Microbiology*, *14*(4), 1009–1023. https://doi.org/10.1111/J.1462-2920.2011.02681.X

Powdery mildew - B.M. Cunfer. (n.d.). Retrieved April 1, 2024, from https://soilcropandmore.info/crops/Wheat/Diseases/PowderyMildew/

Prevedouros, K., Cousins, I. T., Buck, R. C., & Korzeniowski, S. H. (2006). Sources, fate and transport of perfluorocarboxylates. *Environmental Science and Technology*, *40*(1), 32–44. https://doi.org/10.1021/ES0512475

Rice, P. A., Cooper, J., Koh-Fallet, S. E., & Kabadi, S. V. (2021). Comparative analysis of the physicochemical, toxicokinetic, and toxicological properties of ether-PFAS. *Toxicology and Applied Pharmacology*, *422*, 115531. https://doi.org/10.1016/J.TAAP.2021.115531

Rojas-Sandoval, J., & Major, P. (2023). *Plantago major (broad-leaved plaintain) Summary Datasheet Type(s) Preferred Scientific Name Preferred Common Name Summary of Invasiveness*. https://doi.org/10.1079/CABICOMPENDIUM.41814

Roy J. Plunkett | Science History Institute. (n.d.). Retrieved September 26, 2023, from https://sciencehistory.org/education/scientific-biographies/roy-j-plunkett/

Sadia, M., Nollen, I., Helmus, R., Ter Laak, T. L., Béen, F., Praetorius, A., & Van Wezel, A. P. (2023). Occurrence, Fate, and Related Health Risks of PFAS in Raw and Produced Drinking Water. *Environmental Science and Technology*, *57*(8), 3062–3074. https://doi.org/10.1021/ACS.EST.2C06015/ASSET/IMAGES/LARGE/ES2C06015_0006.JPEG

Shahsavari, E., Rouch, D., Khudur, L. S., Thomas, D., Aburto-Medina, A., & Ball, A. S. (2021). Challenges and Current Status of the Biological Treatment of PFAS-Contaminated Soils. *Frontiers in Bioengineering and Biotechnology*, *8*, 602040. https://doi.org/10.3389/FBIOE.2020.602040/BIBTEX

Sharifan, H., Bagheri, M., Wang, D., Burken, J. G., Higgins, C. P., Liang, Y., Liu, J., Schaefer, C. E., & Blotevogel, J. (2021). Fate and transport of per- and polyfluoroalkyl substances (PFASs) in the vadose zone. In *Science of the Total Environment* (Vol. 771). Elsevier B.V. https://doi.org/10.1016/j.scitotenv.2021.145427

Stoiber, T., Evans, S., & Naidenko, O. V. (2020). *Disposal of products and materials containing per-and polyfluoroalkyl substances (PFAS): A cyclical problem*. https://doi.org/10.1016/j.chemosphere.2020.127659

Sunderland, E. M., Hu, X. C., Dassuncao, C., Tokranov, A. K., Wagner, C. C., & Allen, J. G. (2018). A review of the pathways of human exposure to poly- and perfluoroalkyl substances (PFASs) and present understanding of health effects. *Journal of Exposure Science &*

Environmental Epidemiology 2018 29:2, *29*(2), 131–147. https://doi.org/10.1038/s41370-018-0094-1

T Gaines, L. G., & Linda T Gaines, C. G. (2023). Historical and current usage of per- and polyfluoroalkyl substances (PFAS): A literature review. *American Journal of Industrial Medicine*, *66*(5), 353–378. https://doi.org/10.1002/AJIM.23362

The History of Teflon™ Fluoropolymers. (n.d.). Retrieved September 26, 2023, from https://www.teflon.com/en/news-events/history

Trojanowicz, M., Bobrowski, K., Szostek, B., Bojanowska-Czajka, A., Szreder, T., Bartoszewicz, I., & Kulisa, K. (2018). A survey of analytical methods employed for monitoring of Advanced Oxidation/Reduction Processes for decomposition of selected perfluorinated environmental pollutants. *Talanta*, *177*, 122–141. https://doi.org/10.1016/J.TALANTA.2017.09.002

Wang, W., Rhodes, G., Ge, J., Yu, X., Li, H., & Li, H. (2020). *Uptake and accumulation of per-and polyfluoroalkyl substances in plants*. https://doi.org/10.1016/j.chemosphere.2020.127584

Wang, Z., Buser, A. M., Cousins, I. T., Demattio, S., Drost, W., Johansson, O., Ohno, K., Patlewicz, G., Richard, A. M., Walker, G. W., White, G. S., & Leinala, E. (2021). A New OECD Definition for Per- And Polyfluoroalkyl Substances. *Environmental Science and Technology*, *55*(23), 15575–15578. https://doi.org/10.1021/ACS.EST.1C06896/ASSET/IMAGES/LARGE/ES1C06896_0002.JPEG

Young, C. J., Furdui, V. I., Franklin, J., Koerner, R. M., Muir, D. C. G., & Mabury, S. A. (2007). Perfluorinated acids in arctic snow: New evidence for atmospheric formation. *Environmental Science and Technology*, *41*(10), 3455–3461. https://doi.org/10.1021/ES062623

Zenobio, J. E., Salawu, O. A., Han, Z., & Adeleye, A. S. (2022). Adsorption of per- and polyfluoroalkyl substances (PFAS) to containers. *Journal of Hazardous Materials Advances*, *7*, 100130. https://doi.org/10.1016/J.HAZADV.2022.100130

Zhang, W., & Liang, Y. (2020). Removal of eight perfluoroalkyl acids from aqueous solutions by aeration and duckweed. *Science of The Total Environment*, *724*, 138357. https://doi.org/10.1016/J.SCITOTENV.2020.138357

Zhang, W., Zhang, D., Zagorevski, D. V., & Liang, Y. (2019). Exposure of Juncus effusus to seven perfluoroalkyl acids: Uptake, accumulation and phytotoxicity. *Chemosphere*, *233*, 300–308. https://doi.org/10.1016/j.chemosphere.2019.05.258

Zhao, H., Chen, C., Zhang, X., Chen, J., & Quan, X. (2011). *Phytotoxicity of PFOS and PFOA to Brassica chinensis in different Chinese soils*. https://doi.org/10.1016/j.ecoenv.2011.03.007

Appendix

SEM images of all analyzed samples (1= -UV +PFOA, 2= -UV +PFOA, 3= -UV +PFOS, 4= +UV +PFOA, 5= +UV +PFOS, 6 = -UV -PFAS, 7= -UV +PFOA)

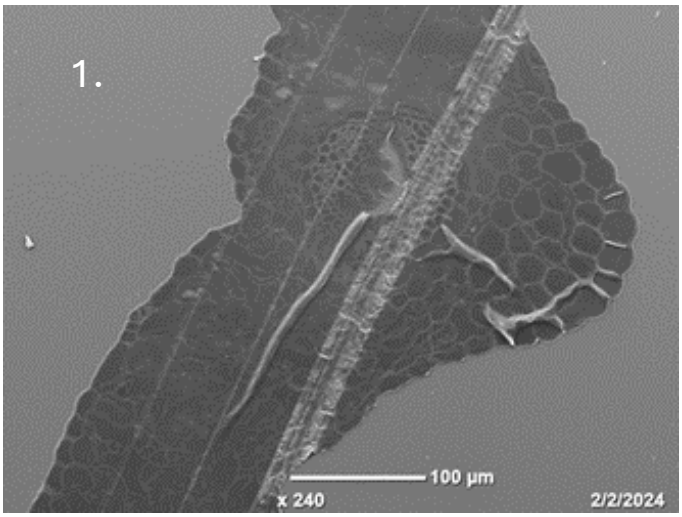

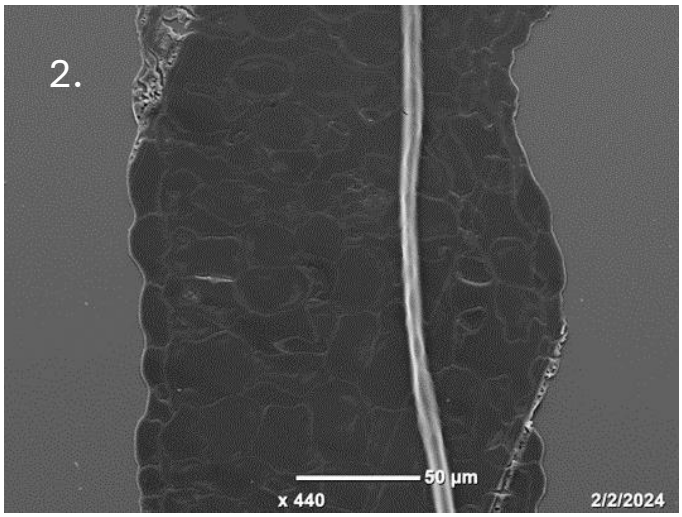

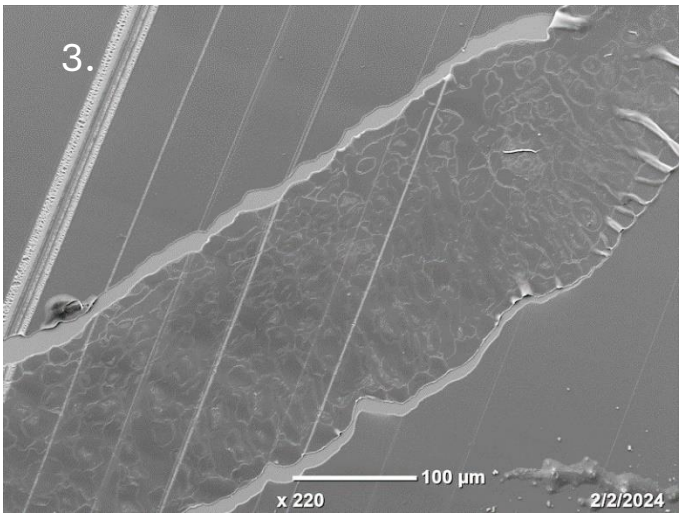

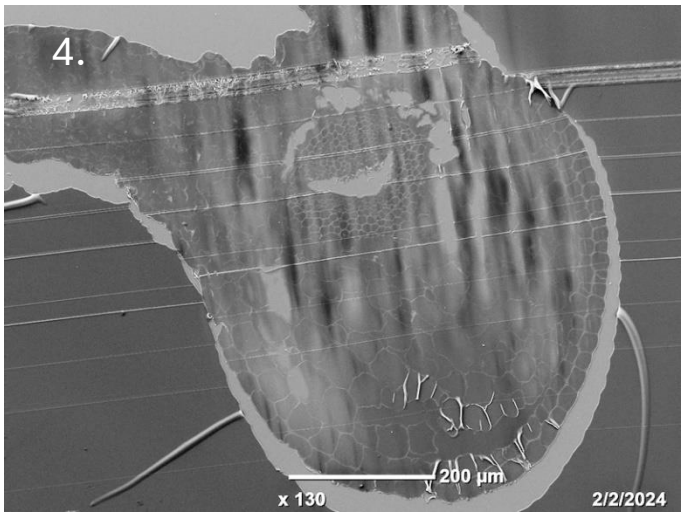

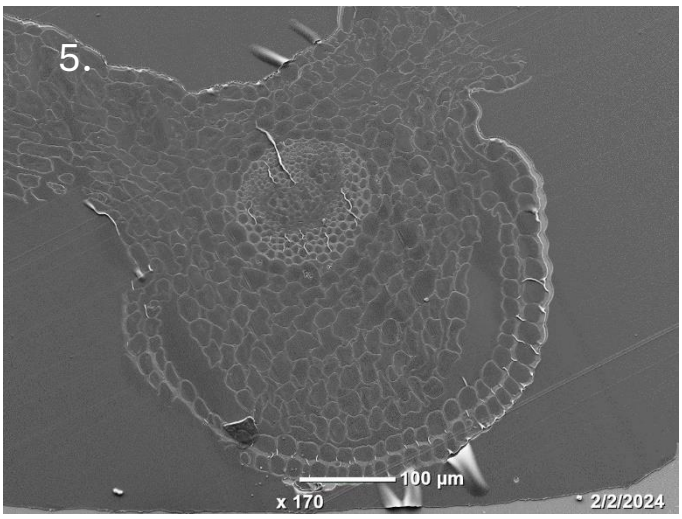

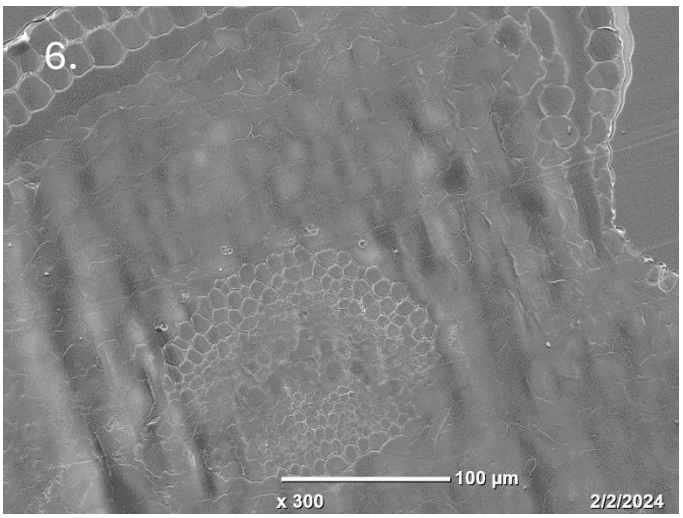

Combined organic matter NanoSIMS images (1= -UV +PFOA, 2= -UV +PFOA, 3= -UV +PFOS, 4= +UV +PFOA, 5= +UV +PFOS, 6 = -UV -PFAS, 7= -UV +PFOA)

1[1]:

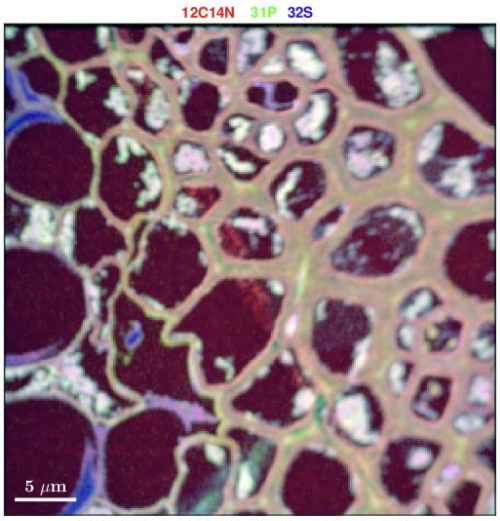

...-02-03-PFASPLANT/2024-02-03-PFASPLANT_1b10/

2[2]:

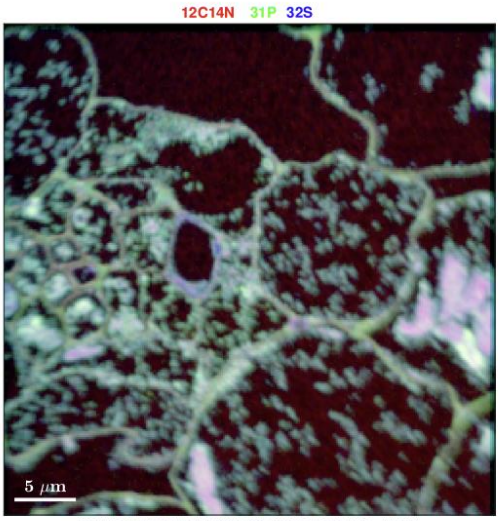

...-02-13-PFASPLANT/2024-02-13-PFASPLANT_1b20/

3[3]:

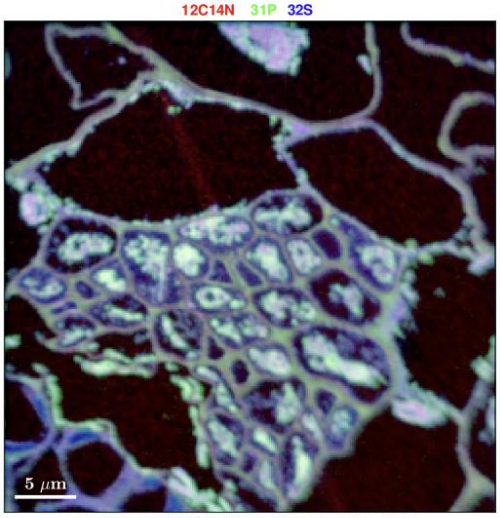

...-02-14-PFASPLANT/2024-02-14-PFASPLANT_1b20/

4[4]:

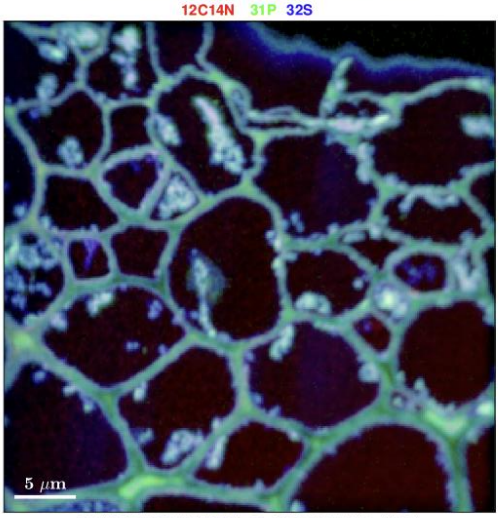

...-02-15-PFASPLANT/2024-02-15-PFASPLANT_1b20/

5[5]:

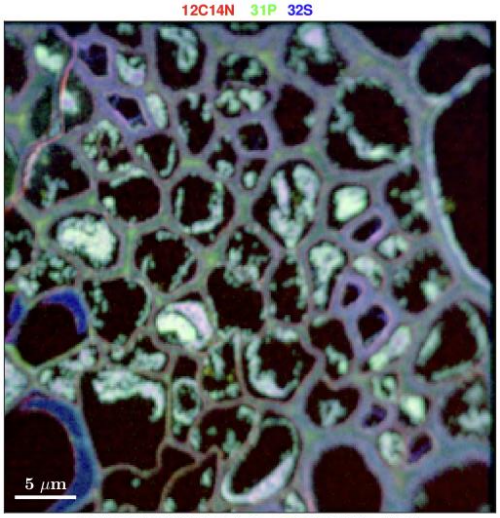

...-02-16-PFASPLANT/2024-02-16-PFASPLANT_1b20/

6[6]:

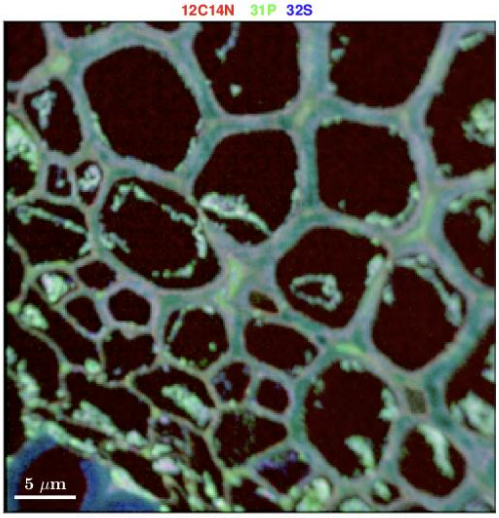

...-02-16-PFASPLANT/2024-02-16-PFASPLANT_2b20/

13/12C ratios of all analyzed samples (1= -UV +PFOA, 2= -UV +PFOA, 3= -UV +PFOS, 4= +UV +PFOA, 5= +UV +PFOS, 6 = -UV -PFAS, 7= -UV +PFOA)

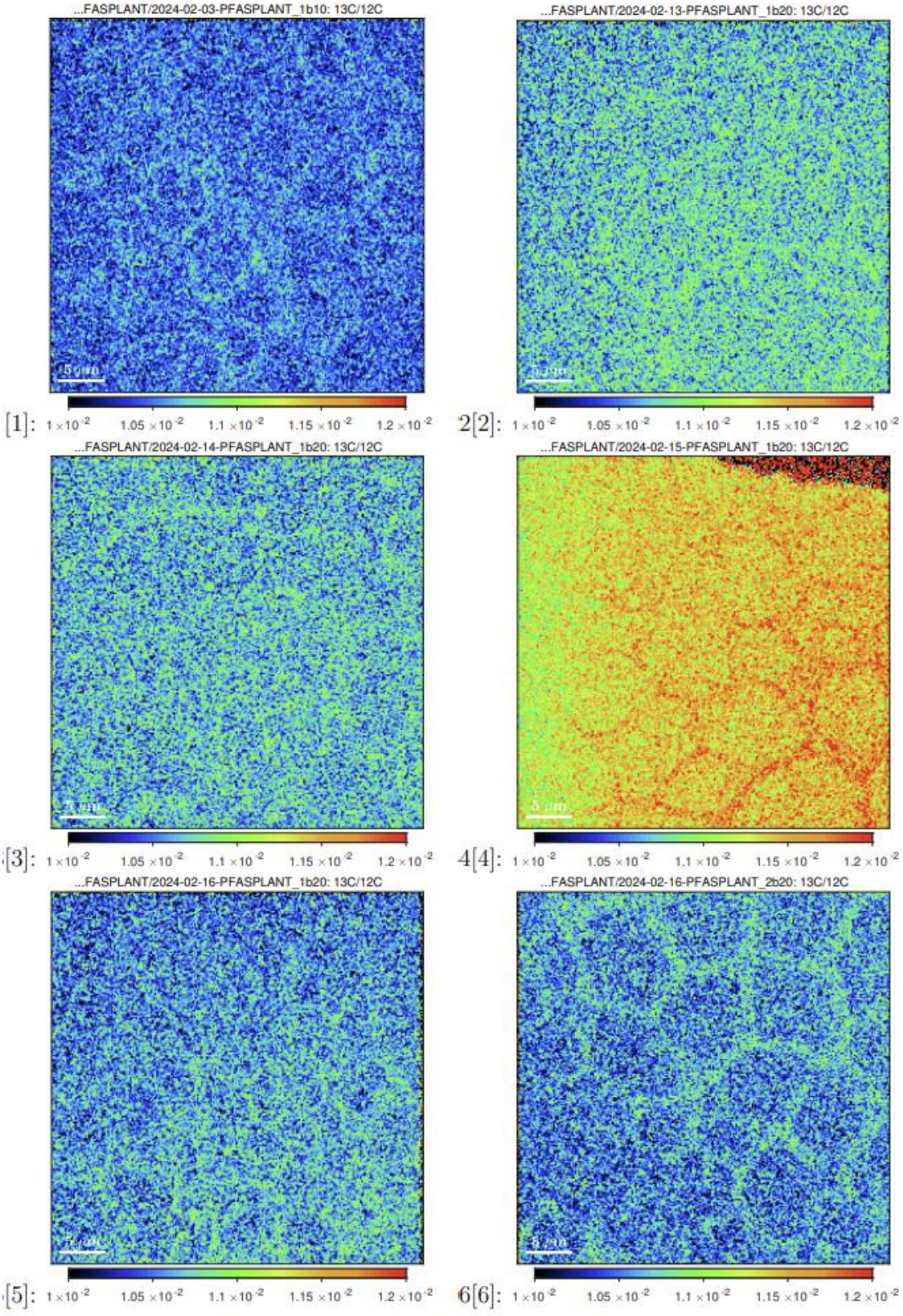

19F/(12C+13C) images of all analyzed samples (1= -UV +PFOA, 2= -UV +PFOA, 3= -UV +PFOS, 4= +UV +PFOA, 5= +UV +PFOS, 6 = -UV -PFAS, 7= -UV +PFOA)